How do the gauche and anomeric effects drive the pseudorotation equilibrium of the pentofuranose moiety of nucleosides?

ARTICLE *in* JOURNAL OF THE AMERICAN CHEMICAL SOCIETY · NOVEMBER 1992

Impact Factor: 12.11 · DOI: 10.1021/ja00074a046

3 AUTHORS, INCLUDING:

Janez Plavec
National Institute of Chemistry
198 PUBLICATIONS **2,571** CITATIONS
SEE PROFILE

Jyoti B Chattopadhyaya
Uppsala University
433 PUBLICATIONS **7,000** CITATIONS
SEE PROFILE

How Do the Gauche and Anomeric Effects Drive the Pseudorotational Equilibrium of the Pentofuranose Moiety of Nucleosides?

Janez Plavec, Weimin Tong, and Jyoti Chattopadhyaya*

Contribution from the Department of Bioorganic Chemistry, Box 581, Biomedical Centre, University of Uppsala, S-751 23 Uppsala, Sweden

Received February 8, 1993®

Abstract: The conformational characteristics of abasic 1-deoxy sugars **1**, **2**, and **3** and pentofuranose moieties in 2′,3′-dideoxy-[ddA (**6**), ddG (**7**), ddC (**8**)], 2′-deoxy-[dA (**9**), dG (**10**), dC (**11**)], and ribo-β-D-nucleosides [Ade (**12**), Gua (**13**), Cyt (**14**)] were established through the analysis of vicinal proton–proton coupling constants extracted from their 500-MHz ^{1}H-NMR spectra recorded at 20 K intervals in the temperature range from 278 to 358 K in D_2O solution. Two novel deuterated analogues of (*S*)-tetrahydrofurfuryl alcohol (**1**), 2-(*S*)-(hydroxymethyl)-4-(*R*)-deuteriotetrahydrofuran (**4**) and 2-(*S*)-(hydroxymethyl)-3-(*S*)-deuteriotetrahydrofuran (**5**), have enabled unequivocal assignment of the complex nine-spin system in its ^{1}H-NMR spectrum. The van't Hoff plots of $[\ln(X_S/X_N)]$ as a function of $1/T$ gave $\Delta H°$ and $\Delta S°$ values of pseudorotational equilibrium in pentofuranoses **1–3** and pentofuranose moieties in nucleosides **6–14**. The values of $\Delta H°$ were dissected into various stereoelectronic effects (gauche versus anomeric effects) of exocyclic substituents on the pentofuranose moiety. Clearly, the gauche effect of the O4′–C4′–C3′–O3′ fragment drives the pseudorotational equilibrium to the S-type conformations, while the gauche effect of the O4′–C1′–C2′–O2′ fragment pushes the pseudorotational equilibrium to the N. These gauche effects are the strongest factors responsible for driving the N ⇄ S pseudorotational equilibrium. The strength of the gauche effect of the O4′–C4′–C3′–O3′ fragment in abasic sugars **1–3** is further tuned by the presence of a heterocyclic base at C1′ in nucleosides **6–14**. The relatively weaker anomeric effect of the heterocyclic base drives the N ⇄ S equilibrium to the N. The assessment of the relative strengths of the anomeric effects in 2′,3′-dideoxy, 2′-deoxy-, and ribo-β-D-nucleosides has shown that the anomeric effect of the cytosine base is stronger than the anomeric effect of the adenine or guanine base. The experimental data suggest that the anomeric effect is considerably reduced as O4′ experiences the electron-withdrawing effect(s) of 2′(3′)-hydroxyls. The differences in the conformational preferences found in purine and pyrimidine ribonucleosides were additionally attributed to the distinct relative strength of the gauche effect of the N–C1′–C2′–O2′ fragment. The preference for the gauche orientation of the N–C1′–C2′–O2′ fragment and therefore S-type sugar conformation is affected by the nature of the purine or pyrimidine glycosyl nitrogen atom.

The pseudorotation concept was introduced to describe the continuous interconversions of puckered forms of the cyclopentane ring.[1] The furanose geometry is conveniently described using the puckering parameters based on the endocyclic torsion angles.[2,3] The Altona–Sundaralingam parameters are the phase angle of pseudorotation (P) and a puckering amplitude (Ψ_m); P defines the part of the ring which is most puckered, and Ψ_m indicates the extent of puckering.[2,3] The pseudorotation cycle, in which P varies from 0° to 360° through a set of 20 distinct twist and envelope conformations can be subdivided into North ($P \approx 0°$), East ($P \approx 90°$), South ($P \approx 180°$), and West ($P \approx 270°$) regions (Scheme I).[2,3] A survey of 178 X-ray crystal structures of nucleosides and nucleotides found nucleosides in both North (N) and South (S) conformations (Scheme I).[4] The first range is centred around P = 18° (C3′-*endo*), whereas the second range is in the South part and is centred around P = 162° (C2′-*endo*). However, there are a few examples of both X-ray[4] and solution[5] structures which have sugar conformations with $P \approx 90°$. These East (E) structures support the hypothesis that the N ⇄ S interconversion proceeds through the E rather than the West (W) conformation. The values of Ψ_m were found in a range from 30° to 46°, and most of them fall within 38.6° ± 3.0°.[4] For 178 β-D-furanoside moieties, the ratio between N and S states in ribonucleosides is approximately 1:1, and for 2′-deoxyribonucleosides, it is 1:3.[4]

Scheme I. Pseudorotational Wheel of the Furanose Ring[a]

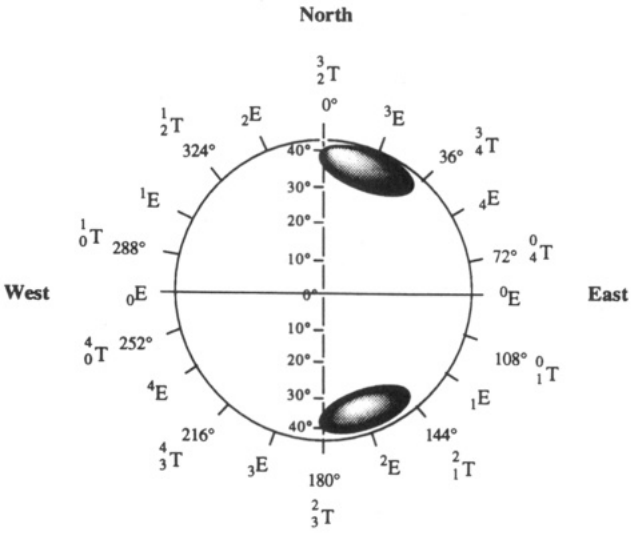

[a] The ring has the Altona–Sundaralingam convention[2,3] and shows the labeling of the characteristic conformers.[7] A survey of X-ray crystal structures show (the shaded zones) that the North conformers are centred around P = 18° (C3′-*endo*) and the South conformers are centred around P = 162° (C2′-*endo*).[4] In both regions, the puckering amplitude (Ψ_m) varies[4,7] from 30° to 46° (the inset scales show the Ψ_m for the furanose ring).

Pseudorotation of cyclopentane can occur without any energy changes, but the presence of endocyclic or exocyclic substituents

* Abstract published in *Advance ACS Abstracts,* September 15, 1993.

(1) Kilpatrick, J. E.; Pitzer, K. S.; Spitzer, R. *J. Am. Chem. Soc.* **1947**, *69*, 2483.
(2) Altona, C.; Sundaralingam, M. *J. Am. Chem. Soc.* **1972**, *94*, 8205.
(3) Altona, C.; Sundaralingam, M. *J. Am. Chem. Soc.* **1973**, *95*, 2333.
(4) de Leeuw, H. P. M.; Haasnoot, C. A. G.; Altona, C. *Isr. J. Chem.* **1980**, *20*, 108.
(5) Hoffmann, R. A.; van Wijk, J.; Leeflang, B. R.; Kamerling, J. P.; Altona, C.; Vliegenthart, J. F. G. *J. Am. Chem. Soc.* **1992**, *114*, 3710.

0002-7863/93/1515-9734$04.00/0

on the cyclopentane ring induces the energy barriers to free pseudorotation.[6,7] The ring oxygen of tetrahydrofuran introduces distinct energy barriers, which result in two localized, symmetrical energy minima at $P = 0°$ and 180°.[6] The preferred conformations of furanose moieties in nucleosides and the relative proportions of various conformers are controlled by the steric and stereoelectronic effects of substituents.[2-38] Systematic surveys of conformational preferences of the 2'-substituted adenosine[27] and uridine[23,24] derivatives in solution have shown that the amount of N conformer increases linearly with electronegativity of 2'-substituent. The sugar conformation is also influenced by modifications of the base,[18] as well as by replacement of the base by -OMe.[32,33] The pseudorotational characteristics of tetrahydrofuran substituted by the CH_2OH group, the base, or other groups are also slightly reflected in the changes of endo- and exocyclic bond distances and bond angles.[7]

Contributions of different steric and stereoelectronic effects of substituents that control the conformational preferences of the pentofuranose moiety have been qualitatively addressed.[2-44] The least favorable conformation in terms of steric interactions alone is W (O4'-*exo*), in which substituents on C2' and C3' are eclipsed and both $-CH_2OH$ and heterocyclic base (bulky substituents) are maximally axial. This corresponds to the well-documented high-energy barrier to pseudorotation in the W region.[39-44] The base has minimum hindrance with the ring when it is in the pseudoequatorial positions of the S conformations, while the 5'-CH_2OH group has minimal hindrance in the N. The qualitative assessment of the steric interactions alone suggests that the preferred furanose conformations for nucleosides should be around $P = 0°$, 18°, 162°, and 180°.[41] The envelope conformers around $P = -18°$ and $P = 198°$ are less favored because either the base or 5'-CH_2OH is axial. However, steric effects alone cannot entirely account for the conformational characteristics of various furanose moieties in (modified) nucleosides.[6,39,40]

The gauche and anomeric stereoelectronic effects are used to understand the conformational behavior of the pentofuranose moiety. The gauche effect is a stabilization of the gauche relative to the trans form upon substitution of X and Y in X-C-C-Y fragments by electronegative groups.[39,40,45,46] Olson *et al.* showed that the preference of the O4'–C4'–C3'–O3' torsion angle for the gauche rather than the trans staggered conformation explains the preference for the S conformers in 2'-deoxyribonucleosides.[39,40] Substitution of the 3'-OH by a group of comparable electronegativity, such as -F[47], $-NO_2$[48] or $-OPO_2^-$[12] has a similar effect. In ribonucleosides, two additional O4'–C1'–C2'–O2' and O2'–C2'–C3'–O3' torsion angles also prefer gauche conformations. Simple model building shows that the orientations of O4'–C1'–C2'–O2' and O4'–C4'–C3'–O3' in the N conformer are gauche and trans, respectively while the reverse is true for the S conformer.[7] In the W conformer, both O4'–C4'–C3'–O3' and O4'–C1'–C2'–O2' are in gauche orientations, and therefore the W is favorable over N and S if only gauche effects of these two fragments are considered.[39,40] The E conformer is unfavorable in comparison with N and S because both O4'–C4'–C3'–O3' and O4'–C1'–C2'–O2' have trans orientations.[7,39,40] The O2'–C2'–C3'–O3' orientation is in an unfavored cis arrangement at $P = 90°$ or 270°, but it tends to take up gauche orientation in N and S conformers. All conformations are, however, energetically high when only the O2'–C2'–C3'–O3' fragment is considered. Therefore, on the basis of gauche effects of O4'–C1'–C2'–O2' and O4'–C4'–C3'–O3' fragments alone, the N- and S-type puckered conformers would be equally populated in ribonucleosides. The anomeric effect was introduced to describe the tendency of an alkoxy group at C1 of a pyranose ring to assume the axial rather than the equatorial orientation despite unfavorable steric interactions.[49] In nucleosides, it describes the tendency of the lone pair on the furanose oxygen to orient antiperiplanar to the nitrogen atom of the base. The anomeric effect is optimal in the O4'-*exo* (W) conformation[41] (antiperiplanar orientation of Lp–O4'–C1'–N), which is unacceptable for steric reasons (*vide supra*). The N-type conformation is energetically favored over S in terms of the anomeric effect alone.

In this work, we have evaluated the relative strengths of the various gauche and anomeric effects that affect the pseudorotational equilibrium. To dissect various contributions of gauche and anomeric effects, various abasic 1-deoxysugars (see supplementary material for experimental details) have been synthesized: (*S*)-tetrahydrofurfuryl alcohol (**1**), 1,2-dideoxy-D-ribofuranose (**2**), and 1-deoxy-D-ribofuranose (**3**). Two deuterated analogues, 2-(*S*)-(hydroxymethyl)-4-(*R*)-deuteriotetrahydrofuran (**4**) and 2-(*S*)-(hydroxymethyl)-3-(*S*)-deuteriotetrahydrofuran (**5**), have also been synthesised to provide unequivocal

(6) Lesyng, B. In *Topics in Nucleic Acid Structure*; Neidle, S., Ed.; Macmillan Press: London, 1987; Part 3, p 71.
(7) Saenger, W. *Principles of Nucleic Acid Structure*; Springer-Verlag: New York, 1984.
(8) Haasnoot, C. A. G.; de Leeuw, F. A. A. M.; Altona, C. *Tetrahedron* **1980**, *36*, 2783.
(9) de Leeuw, F. A. A. M.; Altona, C. *J. Comput. Chem.* **1983**, *4*, 438.
(10) de Leeuw, F. A. A. M.; Altona, C. *QCPE* **1983**, 463.
(11) Haasnoot, C. A. G.; de Leeuw, F. A. A. M.; de Leeuw, H. P. M.; Altona, C. *Org. Magn. Reson.* **1981**, *15*, 43.
(12) Rinkel, L. J.; Altona, C. *J. Biomol. Struct. Dyn.* **1987**, *4*, 621.
(13) de Leeuw, F. A. A. M.; Altona, C. *J. Chem. Soc., Perkin Trans. II* **1982**, 375.
(14) Donders, L. A.; de Leeuw, F. A. A. M.; Altona, C. *Magn. Reson. Chem.* **1989**, *27*, 556.
(15) Altona, C.; Ippel, J. H.; Hoekzema, A. J. A. W.; Erkelens, C.; Groesbeek, G.; Donders, L. A. *Magn. Reson. Chem.* **1989**, *27*, 564.
(16) Diez, E.; Fabian, J. S.; Guilleme, J.; Altona, C.; Donders, L. A. *Mol. Phys.* **1989**, *68*, 49.
(17) Davies, D. B. *Prog. NMR Spectrosc.* **1978**, *12*, 135.
(18) Uhl, W.; Reiner, J.; Gassen, H. G. *Nucleic Acids Res.* **1983**, *11*, 1167.
(19) Ludemann, H. D.; Knopp, G.; Hansske, F.; Robins, M. J. In *Nucleic Acids: The Vectors of Life*; Pullman, B., Jortner, J., Eds.; D. Reidel Publishing Company: Dordrecht, 1983; p 537.
(20) Klimke, G.; Cuno, I.; Ludemann, H. D.; Mengel, R.; Robins, M. J. *Z. Naturforsh.* **1980**, *35*, 853.
(21) Klimke, G.; Cuno, I.; Ludemann, H. D.; Mengel, R.; Robins, M. J. *Naturforsh.* **1980**, *35C*, 865.
(22) Egert, E.; Lindner, H. J.; Hillen, W.; Böhm, M. C. *J. Am. Chem. Soc.* **1980**, *102*, 3707.
(23) Guschlbauer, W.; Jankowski, K. *Nucleic Acids Res.* **1980**, *8*, 1421.
(24) Guschlbauer, W. *Biochim. Biophys. Acta* **1980**, *610*, 47.
(25) Ekiel, I.; Remin, M.; Darzynkiewicz, E.; Shugar, D. *Biochim. Biophys. Acta* **1979**, *562*, 177.
(26) Klimke, G.; Cuno, I.; Ludemann, H. D.; Mengel, R.; Robins, M. J. *Z. Naturforsh.* **1979**, *34C*, 1075.
(27) Uesugi, S.; Miki, H.; Ikehara, M.; Iwahashi, H.; Kyogoku, Y. *Tetrahedron Lett.* **1979**, 4073.
(28) Ekiel, I.; Darzynkiewicz, E.; Dudycz, L.; Shugar, D. *Biochemistry* **1978**, *17*, 1530.
(29) Westhof, E.; Plach, H.; Cuno, I.; Ludemann, H. D. *Nucleic Acids Res.* **1977**, *4*, 939.
(30) Plach, H.; Westhof, E.; Ludemann, H. D.; Mengel, R. *Eur. J. Biochem.* **1977**, *80*, 295.
(31) Imazawa, M.; Ueda, T.; Ukita, T. *Chem. Pharm. Bull.* **1975**, *23*, 604.
(32) Gerlt, J. A.; Youngblood, A. V. *J. Am. Chem. Soc.* **1980**, *102*, 7433.
(33) Raap, J.; van Boom, J. H.; van Lieshout, H. C.; Haasnoot, C. A. G. *J. Am. Chem. Soc.* **1988**, *110*, 2736.
(34) Koole, L. H.; Buck, H. M.; Bazin, H.; Chattopadhyaya, J. *Tetrahedron* **1987**, *43*, 2289.
(35) Koole, L. H.; Buck, H. M.; Nyilas, A.; Chattopadhyaya, J. *Can. J. Chem.* **1987**, *65*, 2089.
(36) Plavec, J.; Koole, L. H.; Chattopadhyaya, J. *J. Biochem. Biophys. Methods* **1992**, *25*, 253.
(37) Kline, P. C.; Serianni, A. S. *J. Am. Chem. Soc.* **1990**, *112*, 7373.
(38) Serianni, A. S.; Barker, R. *J. Org. Chem.* **1984**, *49*, 3292.
(39) Olson, W. K.; Sussman, J. L. *J. Am. Chem. Soc.* **1982**, *104*, 270.
(40) Olson, W. K. *J. Am. Chem. Soc.* **1982**, *104*, 278.
(41) Taylor, E. W.; van Roey, P.; Schinazi, R. F.; Chu, C. K. *Antiviral Chem. Chemother.* **1990**, *1*, 163.
(42) Harvey, S. C.; Prabhakaran, M. *J. Am. Chem. Soc.* **1986**, *108*, 6128.
(43) Pearlman, D. A.; Kim, S.-H. *J. Biomol. Struct. Dyn.* **1985**, *3*, 99.
(44) Saran, A.; Perahia, D.; Pullman, B. *Theor. Chim. Acta* **1973**, *30*, 31.
(45) Phillips, L.; Wray, V. *J. Chem. Soc., Chem. Commun.* **1973**, 90.
(46) Murcko, M. A.; DiPaola, R. A. *J. Am. Chem. Soc.* **1992**, *114*, 10010.
(47) Plavec, J.; Koole, L. H.; Sandström, A.; Chattopadhyaya, J. *Tetrahedron* **1991**, *47*, 7363.
(48) Hossain, N.; Papchikhin, A.; Garg, N.; Fedorov, I.; Chattopadhyaya, J. *Nucleosides Nucleotides* **1993**, *12*, 499.
(49) Deslongchamps, P. *Stereoelectronic Effects in Organic Chemistry*; Pergamon Press: Oxford, 1983.

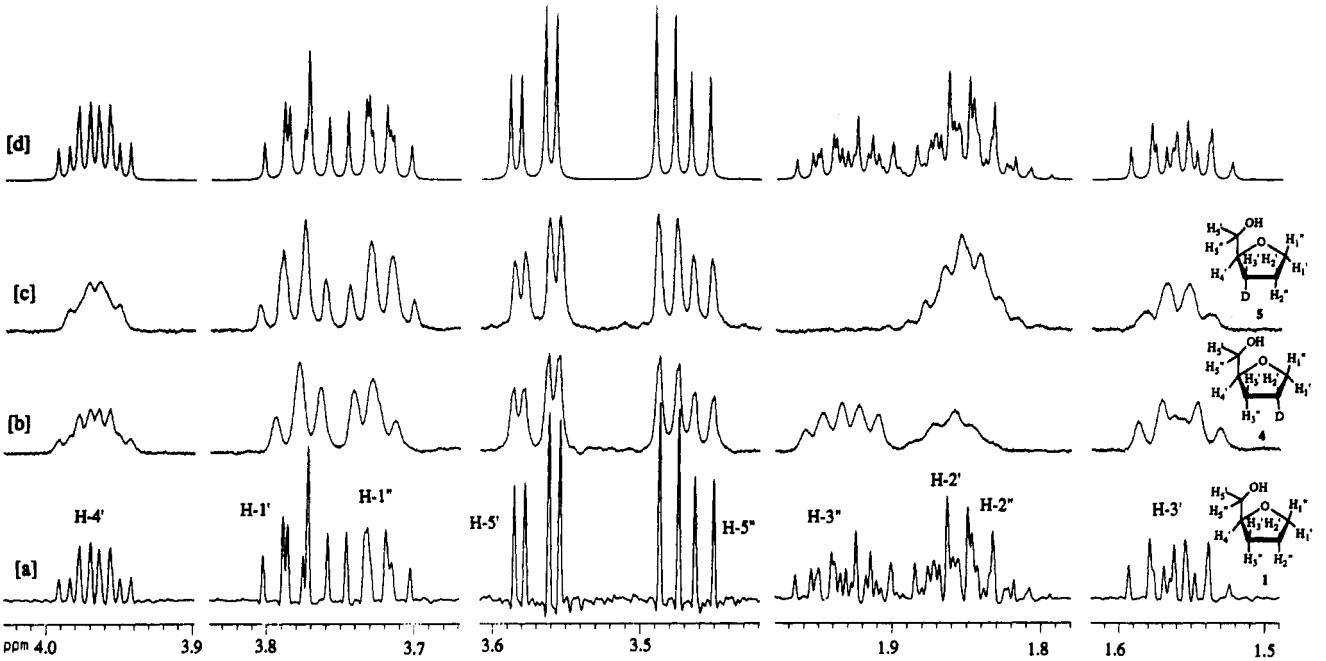

Figure 1. 500-MHz ^{1}H-NMR spectra of (*S*)-tetrahydrofurfuryl alcohol (**1**) [a] and its two deuterated analogues, 2-(*S*)-(hydroxymethyl)-4-(*R*)-dueteriotetrahydrofuran (**4**) [b] and 2-(*S*)-(hydroxymethyl)-3-(*S*)-deuteriotetrahydrofuran (**5**) [c], at 298 K in D_2O. The multiplets are simplified, and the resonances are absent due to stereospecific substitution of H2″ by deuterium in **4** and H3″ in **5** in comparison to the nine-spin system in **1**. Panel d shows the spectrum of **1** obtained by the simulation and iteration procedure by the DAISY program.[60] The assignment of protons on 1-deoxy sugars **1–5** follows the nomenclature for the pentofuranose moieties in β-D-nucleosides.

Chart I

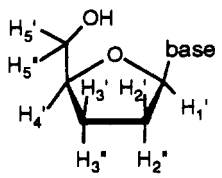

(**6**): base = adenine-9-yl (ddA)
(**7**): base = guanine-9-yl (ddG)
(**8**): base = cytosine-1-yl (ddC)

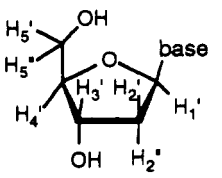

(**9**): base = adenine-9-yl (dA)
(**10**): base = guanine-9-yl (dG)
(**11**): base = cytosine-1-yl (dC)

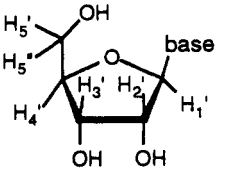

(**12**): base = adenine-9-yl (Ade)
(**13**): base = guanine-9-yl (Gua)
(**14**): base = cytosine-1-yl (Cyt)

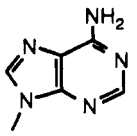

adenine-9-yl

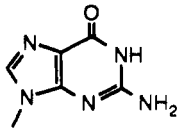

guanine-9-yl

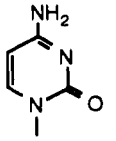

cytosine-1-yl

assignment of the ^{1}H-NMR spectrum of **1** and to all our extraction of proton–proton coupling constants from its nine-spin system (Figure 1).

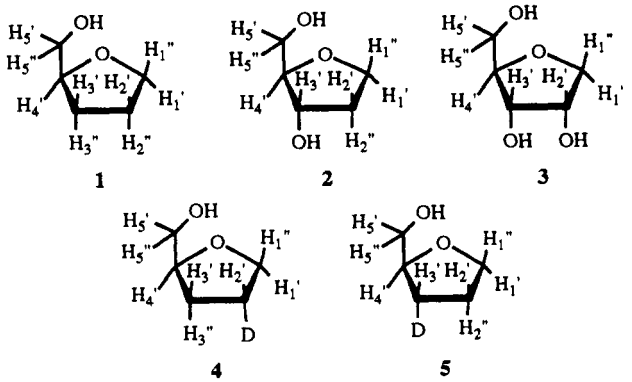

1 **2** **3**

4 **5**

The conformational behavior of abasic sugars **1–3** in D_2O solution have been subsequently determined. These studies let us assess the competing gauche effects of the O4′–C1′–C2′–O2′ and O4′–C4′–C3′–O3′ fragments. By analyzing the preferences for different conformations in 2′,3′-dideoxynucleosides (2′,3′-ddN)[36] [2′,3′-dideoxyadenosine (ddA, **6**), 2′,3′-dideoxyguanosine (ddG, **7**), 2′,3′-dideoxycytosine (ddC, **8**)], 2′-deoxynucleosides (2′-dN) [2′-deoxyadenosine (dA, **9**), 2′-deoxyguanosine (dG, **10**), 2′-deoxycytosine (dC, **11**)], and ribonucleosides (rN) [adenosine (Ade, **12**), guanosine (Gua, **13**), cytidine (Cyt, **14**)], all shown in Chart I, some insights into the anomeric effects of adenine, guanine, and cytosine bases were obtained. The comparison of conformational preferences of pentofuranose in abasic sugars **1–3** and 2′,3′-ddN **6–8**, 2′-dN **9–11**, and rN **12–14** enabled us to quantify the strength of anomeric versus gauche effects that drive the pseudorotational equilibrium.

Conformation of the Pentofuranose Ring. The conformations of the furanose moieties in abasic sugars **1–3** and 2′,3′-ddN [ddA

Table I. $^3J_{H,H}$ Coupling Constants (Hz),[a] Populations of the North Conformers,[b] and Conformers around the C4′–C5′ Bond[c] at Five Distinct Temperatures in the Range from 278 to 358 K

compd	T (K)	$J_{1'2'}$	$J_{1'2''}$	$J_{1''2'}$	$J_{1''2''}$	$J_{2'3'}$	$J_{2'3''}$	$J_{2''3'}$	$J_{2''3''}$	$J_{3'4'}$	$J_{3''4'}$	% N	$J_{4'5'}$	$J_{4'5''}$	% γ^+	% γ^t
1	278	6.9	6.9	5.8	7.6	8.6	5.2	7.4	8.4	7.4	7.2	51.7[d]	3.6	6.5	34	53
	298	6.8	6.9	5.9	7.5	8.6	5.3	7.3	8.4	7.3	7.2	51.2[d]	3.8	6.5	33	52
	318	6.9	6.9	6.0	7.5	8.6	5.2	7.2	8.5	7.2	7.2	50.9[d]	3.9	6.4	33	50
	338	6.9	6.8	6.0	7.5	8.7	5.3	7.1	8.6	7.2	7.2	50.3[d]	4.0	6.4	32	50
	358	6.8	6.9	6.0	7.6	8.7	5.3	7.1	8.5	7.1	7.1	50.9[d]	4.1	6.4	31	50
2	278	9.4	6.6	8.3	3.7	6.2		2.7		3.0		23.6	4.1	6.0	35	45
	298	9.3	6.8	8.3	3.9	6.3		2.8		3.1		25.4	4.2	6.0	34	45
	318	9.0	6.8	8.2	4.0	6.4		3.1		3.1		27.5	4.3	6.0	33	45
	338	8.6	6.9	8.3	4.1	6.4		3.2		3.2		29.6	4.4	6.0	32	45
	358	8.5	6.9	8.3	4.4	6.4		3.2		3.4		31.4	4.4	6.0	32	45
3	278	3.1		4.5		5.0				7.1		64.3[d]	3.1	5.3	51	41
	293	3.0		4.5		5.0				7.1		65.1[d]	3.1	5.3	51	41
	303	3.0		4.5		5.1				7.1		64.8[d]	3.1	5.3	51	41
	313	3.0		4.5		5.1				7.1		64.8[d]	3.1	5.3	51	41
	323	3.1		4.6		5.0				7.0		63.6[d]	3.2	5.4	49	42
dA (**9**)	278	7.8	6.2			6.0		3.1		2.9		24.5	3.1	4.0	65	27
	298	7.7	6.2			6.1		3.3		3.0		26.2	3.3	4.3	60	30
	318	7.3	6.5			6.2		3.5		3.2		29.7	3.5	4.5	56	31
	338	7.2	6.4			6.3		3.7		3.4		31.6	3.6	4.7	53	33
	358	7.1	6.4			6.4		3.8		3.4		32.5	3.7	4.9	50	35
dG (**10**)	278	7.3	6.5			6.2		3.5		3.1		28.0	3.5	4.4	57	30
	298	7.3	6.5			6.3		3.6		3.2		28.8	3.6	4.7	53	33
	318	7.2	6.5			6.5		3.7		3.4		30.4	3.7	4.9	50	35
	338	7.0	6.6			6.6		3.7		3.5		31.7	3.8	5.1	47	37
	358	6.8	6.7			6.8		3.8		3.5		33.1	3.9	5.1	46	37
dC (**11**)	278	7.1	6.3			6.4		4.1		3.9		33.4	3.4	5.2	49	39
	298	6.8	6.5			6.7		4.0		4.0		35.0	3.6	5.2	48	39
	318	6.8	6.5			6.7		4.1		4.0		35.5	3.7	5.3	46	39
	338	6.9	6.5			6.8		4.1		4.1		35.6	3.9	5.4	44	39
	358	6.8	6.5			6.7		4.2		4.1		36.2	3.9	5.4	43	40
Ade (**12**)	278	6.3				5.2				3.1		18.0	2.6	3.3	77	21
	298	6.2				5.3				3.4		20.7	2.8	3.6	72	24
	318	6.0				5.3				3.5		22.8	3.0	3.9	67	27
	338	5.9				5.4				3.8		25.5	3.1	4.1	64	28
	358	5.7				5.4				4.0		28.3	3.2	4.2	62	29
Gua (**13**)	278	6.1				5.2				3.5		21.4	3.0	3.8	68	25
	298	6.0				5.2				3.6		22.9	3.0	4.1	65	29
	318	5.8				5.4				3.8		25.4	3.2	4.2	62	29
	338	5.8				5.4				4.0		26.8	3.3	4.4	59	31
	358	5.7				5.5				4.1		28.1	3.4	4.6	56	33
Cyt (**14**)	278	3.9				5.2				6.2		71.2	2.8	4.3	64	32
	298	4.0				5.3				6.1		69.8	2.9	4.5	61	33
	318	4.1				5.4				6.0		68.5	3.0	4.6	59	34
	338	4.2				5.5				5.9		67.2	3.1	4.7	57	35
	358	4.3				5.6				5.8		65.9	3.2	4.8	55	36

[a] $^3J_{H,H}$ values (±0.1 Hz) are the result of the simulation and iteration procedure by DAISY program package[60] on 1D ^{1}H-NMR spectra recorded at 500 MHz in D_2O; **1**, $^2J_{1'1''} = -8.4$ Hz, $^2J_{2'2''} = -12.3$ Hz, $^2J_{3'3''} = -12.6$ Hz, $^2J_{5'5''} = -11.9$ Hz; **2**, $^2J_{1'1''} = -8.5$ Hz, $^2J_{2'2''} = -13.4$ Hz, $^2J_{5'5''} = -12.0$ Hz; **3**, $^2J_{1'1''} = -10.2$ Hz, $^2J_{5'5''} = -12.4$ Hz. [b] The PSEUROT program (version 5.4)[9,10,14-16] has been used to derive populations at stated temperature as well as geometries of N and S conformers (see Table II). [c] Populations of γ^+ and γ^t conformers were calculated according to ref 61. [d] Population of N conformer is an average from several PSEUROT analyses (eight in the case of **1**, six in the case of **3**, see Figure 3).

(**6**), ddG (**7**), ddC (**8**)], 2′-dN [dA (**9**), dG (**10**), dC (**11**)], and rN [Ade (**12**), Gua (**13**), Cyt (**14**)] were analyzed on the basis of vicinal coupling constants ($^3J_{1'2'}$, $^3J_{1'2''}$, $^3J_{1''2'}$, $^3J_{1''2''}$, $^3J_{2'3'}$, $^3J_{2'3''}$, $^3J_{2''3'}$, $^3J_{2''3''}$, $^3J_{3'4'}$, and $^3J_{3''4'}$) (Table I). The $^3J_{HH}$ were measured at 500 MHz from 278 to 358 K at 20 K intervals in D_2O solution at neutral pH. Note added in proof: The $^3J_{HH}$ have now been also measured at 5 K intervals from 278 to 358 K, and resulting $\Delta H°$ and $\Delta S°$ were comparable wthin the error limits to the ones reported in this paper.

In the solution, the conformation of the furanose ring of nucleosides and nucleotides is interpreted in terms of a two-state equilibrium.[2-36] The generalized Karplus equation links $^3J_{HH}$ coupling constants to corresponding proton–proton torsion angles (Φ_{HH}).[8,14-16] The Φ_{HH} are related to corresponding endocyclic torsion angles (ν_j) by eq 1.[2-4]

$$\Phi_{HH} = A\Psi_m \cos(P + 4\pi(j-2)/5) + B = A\nu_j + B \quad (1)$$

The parameters A and B for ribonucleos(t)ides and 2′-deoxynucleos(t)ides in eq 1 have been developed from the analysis of the conformational properties of sugar residues found in the 178 X-ray crystal structures of various nucleosides.[4,8-13] No relevant X-ray crystal structure is available[50] for **1–3**, and hence it has been mandatory for us to reparametrize the A and B values in eq 1 through *ab initio* optimized geometries in order to analyze the observed $^3J_{HH}$ coupling constants. Twenty-three *ab initio* optimized geometries (Figure 2) for each of the abasic sugars **1–3** were used to correlate the proton–proton torsions with the endocyclic torsion angles. We have performed detailed *ab initio* calculations (GAUSSIAN 92,[51] RHF/3-21G level) with self-consistent reaction field (SCRF) with a dielectric constant of 80 (the radius of spherical cavity around **1–3** was obtained from the molecular volume, and 0.5 Å was added according to the suggestions of Wiberg *et al.*[52]) and compared the resultant A and B parameters with those obtained through calculations in vacuum (Table II), which show virtually no change (for A the average

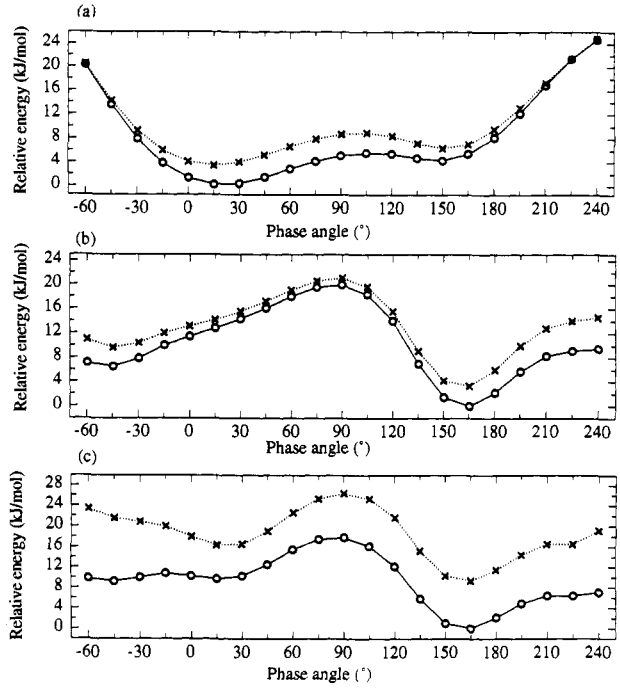

Figure 2. Plot of the relative HF energy (in kJ/mol) as a function of the phase angle of pseudorotation (P) for **1** (panel a), **2** (panel b), and **3** (panel c). The profiles shown above were obtained through optimization of each of the pseudorotamers at the RHF/3-21G level with self-consistent reaction field (SCRF) calculation ($\epsilon = 80$, the cavity radius was obtained from molecular volume and 0.5 Å was added[52]) [GAUSSIAN 92][51] at different P in the range $P = -60°$ to 240° in 15° resolution at $\Psi_m = 39°$. The ν_0[C4′–O4′–C1′–C2′] and ν_4[C3′–C4′–O4′–C1′] were fixed to ensure the conformation with particular P at $\Psi_m = 39°$, while the rest of the molecular was freely optimized. The solid curves [labeled with O) shown in panels a–c correspond to relative SCRF energies, while the dotted curves (labeled with ×) represent relative energies calculated on the same geometries with exclusion of SCRF. In the case of **1**, the completely freely optimized conformer with $P = 20.3°$ ($\psi_m = 38.5°$, γ [O5′–C5′–C4′–C3′] = 61.0°, β [H–O5′–C5′–C4′] = 47.6°, cavity radius = 4.47 Å) is preferred by 4.1 kJ/mol over that with $P = 146.6°$ ($\psi_m = 39.2°$, $\gamma = 61.3°$, $\beta = 54.5°$). For **2**, the conformer with $P = 159.7°$ ($\Psi_m = 40.5°$, $\gamma = 39.8°$, $\beta = 174.8°$, ϵ_3 [C4′–C3′–O3′–H] = 177.6°, cavity radius = 4.54 Å) is preferred over that with $P = -47.6°$ ($\Psi_m = 39.7°$, $\gamma = 49.2°$, $\beta = 175.2°$, $\epsilon_3 = -171.6°$) by 6.6 kJ/mol. For **3**, the conformer with $P = 160.0°$ ($\Psi_m = 38.3°$, $\gamma = 40.1°$, $\beta = 175.9°$, $\epsilon_3 = -76.4°$, ϵ_2 [C3′–C2′–O2′–H] = 31.3°, cavity radius = 4.62 Å) is preferred over that with $P = 22.0°$ ($\Psi_m = 40.4°$, $\gamma = 37.5°$, $\beta = 165.1°$, $\epsilon_3 = -87.6°$, $\epsilon_2 = -39.0°$) by 9.5 kJ/mol.

of the difference = 0.01 with $\sigma = 0.03$, and for B the average of the difference = 0.3° with $\sigma = 1.4°$). In the Figure 2, plots of the relative HF/3-21G energy as a function of the phase angle of pseudorotation (P) for abasic compounds **1**, **2**, and **3** in the range of $-60° < P < 240°$ in 15° resolution at $\Psi_m = 39°$ for 21 optimized conformations are presented. In the above calculations, two endocyclic torsion angles, ν_0[C4′–O4′–C1′–C2′] and ν_4[C3′–C4′–O4′–C1′], were kept frozen,[51] while all other degrees of freedom were optimized. The energy differences between different conformers around the minima in the N and S region are indeed small, especially for **1** (Figure 2a). The range of phase angles within 2 kJ/mol for **1** in the N region extends from $0° < P < 45°$, and in the S (E) region from $100° < P < 170°$. The relative energies shown in the profiles of Figure 2a–c also reflect the energetic variations due to the orientations of exocyclic 5′-CH_2-OH and hydroxy groups.[53]

It is well established that the $^3J_{HH}$ are time-averaged values of the couplings of the individual conformers in a two-state equilibrium.[2–36] Five parameters are needed to describe the N $\rightleftarrows$ S conformational equilibrium: P and ψ_m of both forms and an equilibrium constant, *i.e.*, a mole fraction of one of the conformers. The program PSEUROT calculates the best fit of the five pseudorotational parameters defining the two-state equilibrium to the set of experimental coupling constants.[9,10,14–16] The user provides the input, which consists of (1) the experimental $^3J_{HH}$ measured at various temperature, (2) the substituent electronegativities (shown in the Experimental Section), and (3) the estimated starting values of P_N, P_S, Ψ_m^N, Ψ_m^S, and populations of the South conformer (X_S) at each of the temperatures at which the experimental $^3J_{HH}$ are given. During the iterative optimization procedure, one or more conformational parameters can be constrained to assume a fixed value. The PSEUROT program then back-calculates $^3J_{HH}$ for each conformation generated as a function of P_N, P_S, Ψ_m^N, Ψ_m^S, and X_S and compares it to the experimental $^3J_{HH}$. The quality of the fit is assessed through the calculation of root mean square (rms) deviation between the experimental $^3J_{HH}$ and the back-calculated $^3J_{HH}$ coupling constants (rms = $[1/n\sum[J_i^{expt} - J_i^{calc}(P_N,\Psi_N,P_S,\Psi_S,X_S)]^2]^{1/2}$). The conformational analysis[6,7,11–13] of experimental $^3J_{HH}$ in **1–3**, using the new A and B parameters in eq 1 (*vide infra*), clearly suggests a two-state equilibrium for these abasic sugars. The hyperspace available in the two-state equilibrium has been examined by calculating the rms error as a function of the phase angle in the N range from $-50° < P_N < 40°$ and in the S range $60° < P_S < 200°$ in 5-deg steps. We have furthermore examined the rms error for the accessible ranges of puckering amplitudes, $24° < \Psi_m < 46°$, in 2-deg steps as a function of the phase angle for North and South conformers. These contour plots of rms error obtained by PSEUROT grid analyses of $^3J_{HH}$ for **1**, **2**, and **3** clearly show that these abasic sugars are indeed involved in two-state equilibria (see supplementary material for details): for **1**, ($-40° < P_N < -23°$, $36° < \Psi_m^N < 41°$) $\rightleftarrows$ ($110° < P_E < 123°$, $33° < \Psi_m < 42°$) within rms error of 0.6 Hz; for **2**, ($-21° < P_N < 27°$, $27° < \Psi_m^N < 32°$) $\rightleftarrows$ ($131° < P_S < 135°$, $27° < \Psi_m^S < 31°$) within rms error of 0.3 Hz; for **3**, ($-16° < P_N < 3°$, $37° < \Psi_m^N < 42°$) $\rightleftarrows$ ($76° < P_E < 107°$, $38° < \Psi_m^S < 42°$) within rms error of 0.25 Hz (Table III). The geometries of the conformers of abasic sugars **1–3** and nucleosides **6–14** are shown in Table III, and their populations are presented in Table I. Our conformational analysis was extended by making van't Hoff plots of $\ln(X_S/X_N)$ vs $1/T$ to determine the relative contributions of enthalpy ($\Delta H°$) and the entropy ($\Delta S°$) that drive the conformational equilibria (Figures 3 and 4). Straight lines through experimental data points indeed support the model of a two-state

(50) In the Cambridge Structural Data Base, the positional coordinates for four compounds, **A–D**, are deposited: (**A**, $P = 144.1°$, $\Psi_m = 42.8°$) Vidra, I.; Simon, K.; Institoris, L.; Csoregh, I.; Czugler, M. *Carbohydr. Res.* **1982**, *111*, 41. (**B**, $P = 18.6°$, $\Psi_m = 42.5°$) Irie, M.; Fukuyama, K.; Tsukihara, T.; Katsube, Y.; Morimoto, Y.; Shigemasa, Y.; Nakashima, R. *Acta Crystallogr., Sect. C Cryst. Struct. Commun.* **1985**, *41*, 1814. (**C**, $P = 104.6°$, $\Psi_m = 44.8°$) Lambda, D.; Burden, C.; Mackie, W.; Sheldrick, B. *Carbohydr. Res.* **1986**, *155*, 11. (**D**, $P = 149.7°$, $\Psi_m = 36.0°$ and $P = 212.4°$, $\Psi_m = 31.8°$) Bando, S.; Takano, T.; Tanaka, R.; Iwata, H.; Ishiguro, M. *Acta Crystallogr. Sect. C Cryst. Struct. Commun.* **1990**, *46*, 841.

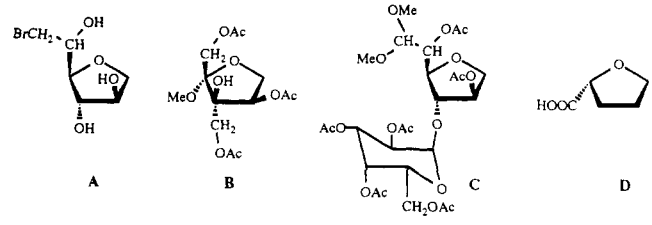

(51) Frish, M. J.; Trucks, G. W.; Head-Gordon, M.; Gill, P. M. W.; Wong, M. W.; Foresman, J. B.; Johnson, B. G.; Schlegel, H. B.; Robb, M. A.; Replogle, E. S.; Gomperts, R.; Andres, J. L.; Raghavachari, K.; Binkley, J. S.; Gonzales, C.; Martin, R. L.; Fox, D. J.; Defrees, D. J.; Baker, J.; Stewart, J. J. P.; Pople, J. A. *Gaussian 92*, Revision A; Gaussian, Inc.: Pittsburgh, PA, 1992.

(52) Wong, M. W.; Frisch, M. J.; Wiberg, K. B. *J. Am. Chem. Soc.* **1991**, *113*, 4776.

(53) It was shown before that the orientation of hydroxy groups can have a dramatic impact on puckering: Lesyng, B.; Saenger, W. *Carbohydr. Res.* **1984**, *133*, 187.

Table II. *A,B* Parameters[a] Correlating Proton–Proton and Endocyclic Torsion Angles Based on Torsion Angles from HF/3-21G Optimized Geometries for Abasic Sugars **1**–**3**[b,c,d]

	compd **1**		compd **2**		compd **3**	
Φ_{HH}	A (A^c)	B (B^c)	A (A^c)	B (B^c)	A (A^c)	B (B^c)
$\Phi_{1'2'}$	1.11 (1.08)	122.2° (123.1°)	1.14 (1.10)	121.5° (122.9°)	1.09 (1.07)	121.9° (122.8°)
$\Phi_{1'2''}$	1.08 (1.06)	0.0° (1.3°)	1.09 (1.10)	−2.6° (−0.4°)		
$\Phi_{1''2'}$	1.09 (1.08)	−1.6° (−0.7°)	1.11 (1.10)	−2.9° (−1.4°)	1.07 (1.08)	−2.1° (−0.7°)
$\Phi_{1''2''}$	1.06 (1.06)	−123.8° (−122.5°)	1.06 (1.10)	−127.0° (−124.7°)		
$\Phi_{2'3'}$	1.15 (1.15)	0.4° (0.6°)	1.17 (1.17)	0.5° (0.2°)	1.16 (1.15)	1.7° (−0.8°)
$\Phi_{2'3''}$	1.12 (1.13)	−122.2° (−121.8°)				
$\Phi_{2''3'}$	1.13 (1.14)	122.8° (122.7°)	1.13 (1.15)	122.3° (122.0°)		
$\Phi_{2''3''}$	1.10 (1.12)	0.1° (0.3°)				
$\Phi_{3'4'}$	1.09 (1.03)	−121.5° (−123.4°)	1.08 (1.02)	−120.1° (−122.6°)	1.13 (1.05)	−121.5° (−121.7°)
$\Phi_{3''4'}$	1.08 (1.04)	−0.1° (−2.0°)				

[a] The relationship between proton–proton torsion angles (Φ_{HH}) an endocyclic torsion angles (ν_j) is $\Phi_{HH} = A\nu_j + B$. For **1**, for example $\Phi_{1'2'} = 1.11\nu_1 + 122.2°$. [b] The *ab initio* calculations at RHF SCF/3-21G level were used[51,62] for complete geometry optimization of N and S conformers of **1** (converged to $P = 16.0°$, $\Psi_m = 38.0°$ and $P = 150.2°$, $\Psi_m = 38.9°$), **2** ($P = 27.1°$, $\Psi_m = 40.1°$ and $P = 155.2°$, $\Psi_m = 42.0°$), and **3** ($P = 18.1°$, $\Psi_m = 45.7°$ and $P = 152.4°$, $\Psi_m = 42.1°$). For each of these six structures, Φ_{HH} and ν_j were extracted and used to calculate parameters A and B. [c] Φ_{HH} and ν_j were extracted from 23 HF/3-21G SCRF (dielectric constant = 80) optimized geometries of **1**–**3** (see Figures 3–5); 21 optimizations for each of the abasic sugars **1**–**3** (see text) were performed with P fixed in the range of $-60° < P < 240°$ in 15° resolution at $\Psi_m = 39°$ (Figure 2), while two conformations from the minima in the N and S region were completely freely optimized for **1** (converged to $P = 20.3°$, $\Psi_m = 38.5°$ and $P = 146.6°$, $\Psi_m = 39.2°$), **2** (converged to $P = -47.6°$, $\Psi_m = 39.7°$ and $P = 159.7°$, $\Psi_m = 40.5°$), and **3** (converged to $P = 22.0°$, $\Psi_m = 40.4°$ and $P = 160.0°$, $\Psi_m = 38.3°$). [d] The average of the difference between the two sets of A and B is 0.01 for A, with $\sigma = 0.03$, and 0.3° for B, with $\sigma = 1.4°$.

Table III. Optimized Pseudorotational Parameters and Errors of Pseudorotational Analyses[a] Based on $^3J_{HH}$ Measured at Five Distinct Temperatures in the Range from 278 to 358 K

compd	P_N (deg)	Ψ_N (deg)	P_S (deg)	Ψ_S (deg)	rms (Hz)[b]	ΔJ_{max} (Hz)
1	−40 to −23	35–42	110–123	35–42	0.6	$\Delta J_{1''2''} = 1.0$, $\Delta J_{1'2'}$, $\Delta J_{2'3''} = 0.7$, $\Delta J_{2'3'} = 0.6$
2	5	29	142	29	0.2	$\Delta J_{1'2'} = \Delta J_{1''2'} = \Delta J_{1''2''} = 0.4$
3	−16 to 3	37–42	76–107	37–42	0.25	$\Delta J_{1''2'} = \Delta J_{2'3'} = 0.2$
ddA (**6**)[d]	1	34	160	34[c]	0.5	1.1
ddG (**7**)[d]	2	34	163	34[c]	0.4	0.8
ddC (**8**)[d]	11	35	154	35[c]	0.4	1.0
dA (**9**)	10[c]	35[c]	155	32	0.2	$\Delta J_{1'2''} = 0.4$, $\Delta J_{1'2'}$, $\Delta J_{2''3'} = 0.3$
dG (**10**)	10[c]	35[c]	153	29	0.3	$\Delta J_{1'2'}$, $\Delta J_{1'2''}$, $\Delta J_{2'3'}$, $\Delta J_{2''3'} = 0.4$
dC (**11**)	10[c]	35[c]	142	31	0.2	$\Delta J_{2''3'} = 0.4$
Ade (**12**)	9[c]	39[c]	142	30	0.1	$\Delta J_{2'3'} = 0.2$
Gua (**13**)	9[c]	39[c]	139	30	0.1	$\Delta J_{2'3'} = 0.2$
Cyt (**14**)	47	33	161[c]	36[c]	0.1	$\Delta J_{2'3'} = 0.2$

[a] The least-squares minimization program PSEUROT (version 5.4) has been used.[9,10,14–16] For $^3J_{HH}$ and equilibrium populations of N ⇄ S equilibrium at various temperatures see Table I. Analyses of $^3J_{HH}$ of **1**–**3** have been performed through grid searches. [b] The rms deviation represents the deviation of calculated and experimental $^3J_{HH}$: $\text{rms} = [1/n\sum[J_i^{expt} - J_i^{theor}(P_N,\Psi_N,P_S,\Psi_S,X_S)]^2]^{1/2}$. [c] The pseudorotational parameter was kept fixed during optimization. [d] Data from ref 36.

conformational equilibrium[2–41] in the furanose rings of **1**–**3**, 2′,3′-ddN [ddA (**6**), ddG (**7**), ddC (**8**)], 2′-dN [dA (**9**), dG (**10**), dC (**11**)], and rN [Ade (**12**), Gua (**13**), Cyt (**14**)].

Assessment of Stereoelectronic Effects of Substituents on the Conformational Behavior of the Pentofuranose Moiety. We have evaluated the conformational characteristics of pentofuranoses **1**, **2**, and **3** and nucleosides **6**–**14** in four stages according to Scheme II.

Level I: Gauche Effects. A simple model building of abasic sugar **1** shows that orientation of the 5′-CH_2OH is pseudoequatorial in the N-type conformation and pseudoaxial in the S-type.[7,41] The preference of the 5′-CH_2OH group to occupy pseudoequatorial orientation is manifested in the positive value of $\Delta H°$ [0.4 ± 0.3 kJ/mol] and therefore drives the pseudorotational equilibrium of pentofuranose **1** toward N conformation (Table IV). The 3′-OH in abasic sugar **2** drives the pseudorotational equilibrium toward S (Table I), which is reflected in its largely negative $\Delta H°$ [−4.2 ± 0.2 kJ/mol] in comparison with that of **1** (Table IV). Comparison of $\Delta H°$ values in **1** and **2** suggests that the strength of the gauche effect of the O4′–C4′–C3′–O3′ fragment is −4.6 ± 0.5 kJ/mol. The entropy term [$-T\Delta S° = 1.5$ ± 0.3 kJ/mol] prefers the N conformer in **2**, but it is weaker at 298 K than the counteracting contribution of $\Delta H°$ [−4.2 ± 0.2 kJ/mol] (Table IV). Comparison of $\Delta H°$ values in **2** and **3** suggests that the strength of the gauche effect of the O4′–C1′–C2′–O2′ fragment is +4.5 ± 1.0 kJ/mol. The $\Delta H°$ values are comparable in **1** [0.4 ± 0.3 kJ/mol] and **3** [0.3 ± 0.8 kJ/mol] (Table IV), which proves that in **3** the gauche effects of the O4′–C1′–C2′–O2′ and O4′–C4′–C3′–O3′ fragments effectively cancel each other and the observed $\Delta H°$ value is the consequence of pseudoequatorial over pseudoaxial preference of 5′-CH_2OH group. The entropy term at 298 K [$-T\Delta S° = 1.1 \pm 1.1$ kJ/mol] is, however, driving the pseudorotational equilibrium in **3** to the N (see Table IV and note 54). Subtraction of $\Delta H°$ values in 2′-dN **9**–**11** and 2′,3′-ddN **6**–**8**, respectively gives an estimate of the strength of the O4′–C4′–C3′–O3′ gauche effect: −8.3 kJ/mol for the dA (**9**)/ddA (**6**) pair, −6.7 kJ/mol for the dG (**10**)/ddG

(54) A set of pseudorotational analyses on **1**–**3** was performed without consideration of coupling constants involving H1″, *i.e.*, $J_{1''2'}$ and $J_{1''2''}$ in **1** and **2** and $J_{1''2'}$ in **3**, as the errors in the individual $^3J_{HH}$ during PSEUROT analysis were the largest for these coupling constants (Table III). In the case of **1**, the geometries of the two pseudorotamers changed only slightly, and therefore similar N ⇄ E pseudorotational equilibrium ($P_I = -7°$, $\Psi_m = 32°$ and $P_{II} = 117°$, $\Psi_m = 39°$; rms = 0.3 Hz) was obtained (compare Table III). The populations of both conformers of **1** at five temperatures gave similar value for enthalpy ($\Delta H° = 0.6 \pm 0.3$ kJ/mol) and a slightly larger value for entropy ($\Delta S° = 2.5 \pm 0.8$ J/K·mol) in comparison to the values presented in Table IV. The abasic sugar **2** is involved in the equilibrium between $P_I = 0°$, $\Psi_m = 32°$ and $P_{II} = 134°$, $\Psi_m = 32°$ (five $^3J_{HH}$ values versus five unknowns, the geometry of the minor conformer was fixed, rms <0.1 Hz). The differences in the values of $\Delta H°$ and $\Delta S°$ for **2** were negligible in comparison to the values in Table IV. In the case of **3**, the system becomes even more underdetermined (three experimental $^3J_{HH}$ values versus five pseudorotational parameters, see text). The geometry of the minor S conformer of **3** was constrained at $P_S = 160°$, $\Psi_m = 38°$ and the major conformer (87% at 293 K) was characterized by $P_N = 36°$, $\Psi_m = 32°$ (rms <0.1 Hz). The higher population of the N conformer in **3** compared to that from the pseudorotational analysis when all four $^3J_{HH}$ values were used is due to the higher value of entropy ($\Delta S° = -13.3 \pm 6.7$ J/K·mol), while the change in the value of enthalpy ($\Delta H° = 0.5 \pm 1.7$ kJ/mol) is well inside the error limits (compare Table IV).

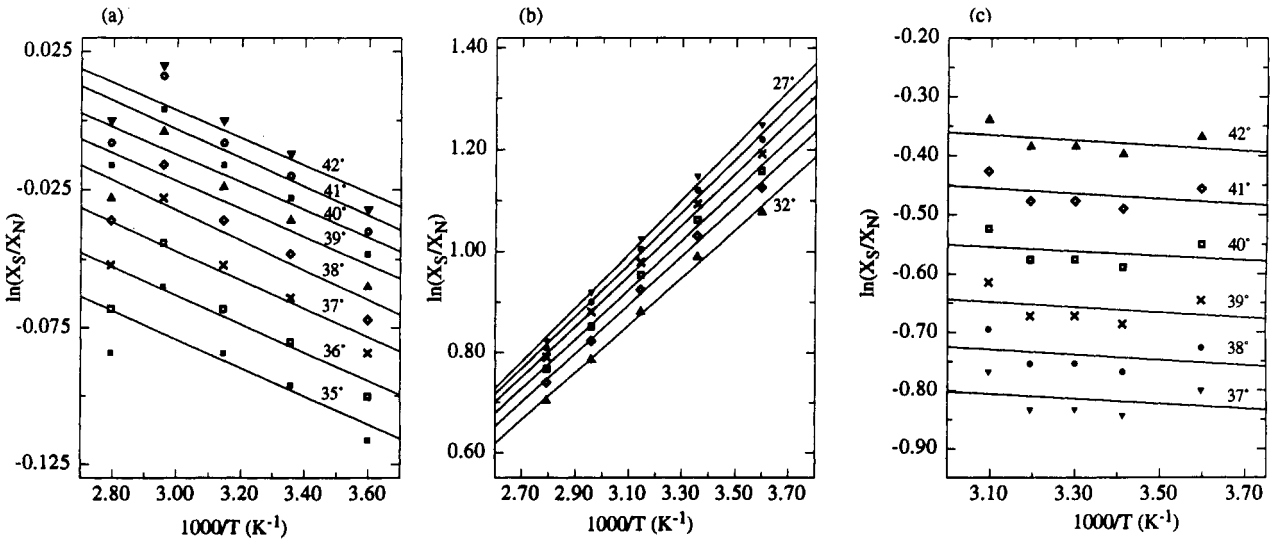

Figure 3. van't Hoff plots of $\ln(X_S/X_N)$ as a function of $1000/T$. The mole fractions of S and N conformers for **1** (panel a), **2** (panel b), and **3** (panel c) were determined by PSEUROT analyses of $^3J_{HH}$ measured at five temperatures in the range from 278 to 358 K by fixing the Ψ_m of both conformers in the range of $35° < \Psi_m < 42°$ for **1**, $27° < \Psi_m < 32°$ for **2**, and $37° < \Psi_m < 42°$ for **3** in 1-deg steps. From the slopes and the intercepts with ordinate of the straight lines computed for the data set for **1** [all eight slopes are –0.05 K, intercepts are 0.08 (Ψ_m = 35°), 0.09 (Ψ_m = 36°), 0.11 (Ψ_m = 37°), 0.13 (Ψ_m = 38°), 0.13 (Ψ_m = 39°), 0.14 (Ψ_m = 40°), 0.15 (Ψ_m = 41°), 0.15 (Ψ_m = 42°)], **2** [0.53 K and –0.66 (Ψ_m = 27°), 0.52 K and –0.63 (Ψ_m = 28°), 0.50 K and –0.61 (Ψ_m = 29°), 0.49 K and –0.60 (Ψ_m = 30°), 0.49 K and –0.61 (Ψ_m = 31°), 0.47 K and –0.61 (Ψ_m = 32°)], and **3** [all six slopes are –0.04 K, intercepts are –0.67 (Ψ_m = 37°), –0.59 (Ψ_m = 38°), –0.51 (Ψ_m = 39°), –0.44 (Ψ_m = 40°), –0.32 (Ψ_m = 41°), –0.23 (Ψ_m = 42°)], $\Delta H°$ and $\Delta S°$ were calculated, respectively, according to the relation $\ln(X_S/X_N) = -(\Delta H°/R)(1000/T) + \Delta S°/R$. The values of $\Delta H°$ for **1**, **2**, and **3** are 0.4, –4.2 (σ = 0.2 calculated from the six slopes in b), and 0.3 kJ/mol, respectively, while the average $\Delta S°$ values for **1**, **2**, and **3** are 1.0 (σ = 0.2 calculated from the eight intercepts in a), –5.2 (σ = 0.2 calculated from the six intercepts in b), and –3.8 J/K·mol (σ = 1.3 calculated from the six intercepts in c), respectively. The $\Delta H°$ and $\Delta S°$ values, together with the error estimates calculated from 90% confidence limits, are presented in Table 4.

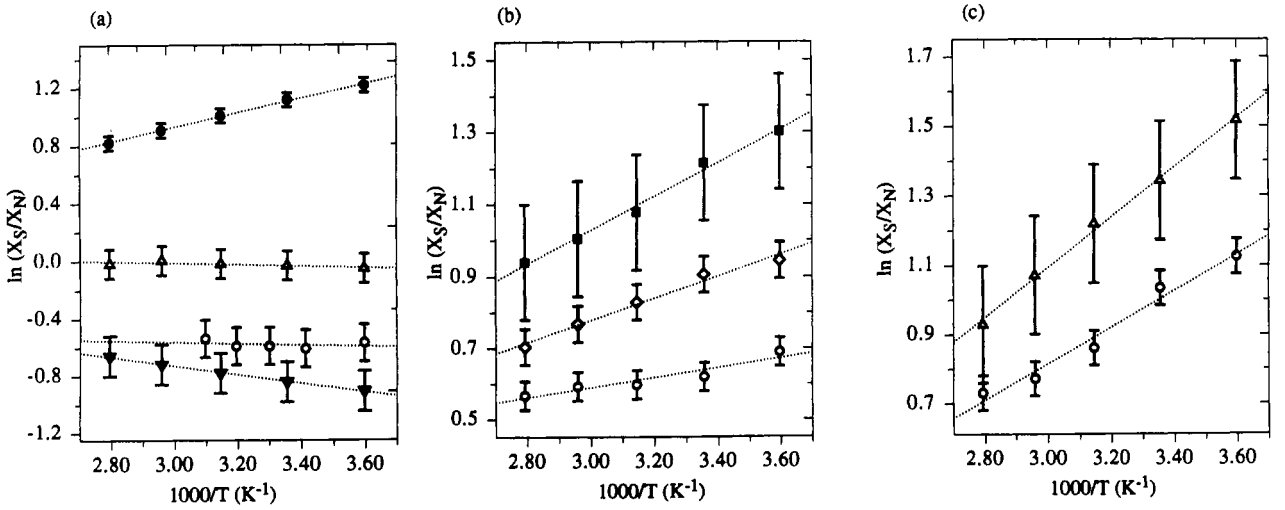

Figure 4. van't Hoff plots of $\ln(X_S/X_N)$ as a function of $1000/T$. The mole fractions of S and N conformers were determined through analysis of $^3J_{HH}$ with the PSEUROT program[6,7,11-13] at five temperatures in the range from 278 to 358 K (Table I). From the slope and the intercept with ordinate of the straight lines, $\Delta H°$ and $\Delta S°$ were calculated for N ⇄ S conformational equilibrium, respectively, according to the relation $\ln(X_S/X_N) = -(\Delta H°/R)(1000/T) + \Delta S°/R$. In panel a, the slopes and the intercepts of the least-squares fit to the experimental data points are shown for **1** (△), slope = –0.05 K, intercept = +0.1; **2** (●), slope = +0.5 K, intercept = –0.6; **3** (○), slope = –0.05 K, intercept = –0.4; and Cyt (**14**) (▼), slope = –0.3 K, intercept = +0.2. The error bars in panel a correspond to 3% error in the population of N and S conformers for Cyt (**14**). For **1**, **2**, and **3**, the data and error bars correspond to the average population at each temperature (Table I) and the variation of the population shown in Figure 3. In panel b, the data for Gua (**13**) (■), slope = +0.5 K, intercept = –0.4; dG (**10**) (◇), slope = +0.3 K, intercept = –0.1, and dC (**11**) (○), slope = +0.1 K, intercept = +0.2, are presented. The error bars in panel b correspond to 3% error in population for Gua (**13**) and 1% error for dG (**10**) and dC (**11**). In panel c, the data for Ade (**12**) (△), slope = +0.7 K, intercept = –1.1, and dA (**9**) (○), slope = +0.5 K, intercept = –0.8, are presented. The error bars for Ade (**12**) and dA (**9**) in panel c correspond to 3% and 1% error in population, respectively.

(**7**) pair, and –7.7 kJ/mol for the dC (**11**)/ddC (**8**) pair. The values differ from the estimates obtained by comparing **1** and **2**, which suggests that the stereoelectronic effects of substituents on pentofuranose moiety are strongly correlated (*vide infra*). The cumulative gauche effects of the O4′–C1′–C2′–O2′ and N–C1′–C2′–O2′ fragments were obtained through the comparison of $\Delta H°$ values in N **12–14** with 2′-dN **9–11**: –1.6 kJ/mol in the Ade (**12**)/dA (**9**) pair, –1.7 kJ/mol in the Gua (**13**)/dG (**10**) pair, and +3.3 kJ/mol in the Cyt (**14**)/dC (**11**) pair. Subtraction of the gauche effect of the O4′–C1′–C2′–O2′ fragment (assuming that it is equal in the strength to the gauche effect of the O4′–C4′–C3′–O3′ fragment, which is evident from comparison of $\Delta H°$ values between **1**/**2** and **2**/**3**) yields the estimate for the N–C1′–C2′–O2′ gauche effect in **12–14**: –9.9 kJ/mol in the case of adenine as a base, –8.4 kJ/mol with guanine, and –4.4 kJ/mol with cytosine.

Scheme II. Elucidation of Mechanism of Stereoelectronic Effects That Drive Pseudorotational Equilibrium in D-Pentofuranoses and β-D-Nucleosides

Level I

Conformational behavior of abasic sugars **1**, **2**, and **3** and 2′-dN **9–11** with respect to 2′,3′-ddN **6–8**

Estimation of gauche effects

↓

Level II

Conformational behavior of 2′,3′-ddN **6–8** with respect to **1**, 2′-dN **9–11** with respect to **2**, and rN **12–14** with respect to **3**

Estimation of anomeric effects

↓

Level III

Conformational behavior of 2′,3′-ddN **6–8**, 2′-dN **9–11**, and abasic sugars **1** and **2**

Both gauche and anomeric effects are functioning

↓

Level IV

Conformational behavior of 2′,3′-ddN **6–8**, 2′-dN **9–11**, rN **12–14**, and abasic sugars **1–3**

Anomeric and various gauche effects are functioning

Table IV. Values for $\Delta H°$ and $\Delta S°$ of the N ⇄ S Conformational Equilibria as Obtained through van't Hoff Plots, $\Delta G°$, and Population of the N Conformer at 298 K

compd	ΔH^a (kJ/mol)	ΔS^a (J/K·mol)	$-T\Delta S^b$ (kJ/mol)	ΔG^{298} (kJ/mol)	% N^c (298 K)
1	0.4 ± 0.3	1.0 ± 1.0	−0.3	0.1	51
2	−4.2 ± 0.2	−5.2 ± 0.9	1.5	−2.7	25
3	0.3 ± 0.8	−3.8 ± 3.7	1.1	1.4	64
ddA (**6**)^d	4.1 ± 0.2	5.2 ± 0.6	−1.6	2.6	74
ddG (**7**)^d	4.2 ± 0.2	5.2 ± 0.7	−1.6	2.7	75
ddC (**8**)^d	6.9 ± 0.3	12.7 ± 1.0	−3.8	3.1	78
dA (**9**)	−4.2 ± 0.6	−6.7 ± 2.5	2.0	−2.2	
dG (**10**)	−2.5 ± 0.3	−0.8 ± 0.8	0.2	−2.3	28
dC (**11**)	−0.8 ± 0.4	1.7 ± 0.8	−0.5	−1.3	37
Ade (**12**)	−5.8 ± 0.3	−9.1 ± 0.7	2.7	−3.1	22
Gua (**13**)	−4.2 ± 0.3	−3.3 ± 0.9	1.0	−3.2	21
Cyt (**14**)	2.5 ± 0.1	1.7 ± 0.3	−0.5	2.0	69

^{a} $\Delta H°$ and $\Delta S°$ were calculated from the slope and the intercept of the line obtained through the least-squares fitting procedure of $\ln(X_S/X_N)$ to the reciprocal of temperature: $\ln(X_S/X_N) = -(\Delta H°/R)(1000/T) + \Delta S°/R$ (Figures 3 and 4). The 90% confidence limits of the slope and the intercept of the line were calculated assuming that experimental data are normally distributed, all with the same standard deviation (program proFit 4.0, Quantum Soft, Switzerland). These values were used to calculate the error estimates for $\Delta H°$ and $\Delta S°$. ^{b} This term illustrates the contribution of entropy term to the Gibbs free energy at 298 K ($\Delta G° = \Delta H° - T\Delta S°$). ^{c} The population of the N conformer at 298 K was calculated through the relation % N = $100/[\exp(-\Delta G^{298}/RT) + 1]$. R is the gas constant (8.314 J/K·mol). ^{d} Data from ref 36.

Level II: Anomeric Effects. Subtraction of $\Delta H°$ for **1** from the values of $\Delta H°$ in 2′,3′-ddN **6–8** (Table IV) has shown that the anomeric effect of cytosine is stronger [+6.5 ± 0.6 kJ/mol] than those of adenine [+3.7 ± 0.5 kJ/mol] and guanine [+3.8 ± 0.5 kJ/mol] bases. An analogous comparison of the $\Delta H°$ values of **2** with 2′-dN **9–11** shows that the anomeric effect of adenine [0 ± 0.8 kJ/mol] and guanine [+1.7 ± 0.5 kJ/mol] bases is weaker than that of cytosine base [+3.4 ± 0.6 kJ/mol]. Clearly, the gauche effect of the O4′–C4′–C3′–O3′ fragment is much stronger than the anomeric effect in 2′-dN (**9–11**) and drives the N ⇄ S pseudorotational equilibrium to the S. A correlation of $\Delta H°$ values in **3** and rN **12–14** is more complex because of the contribution from three different gauche effects (O4′–C4′–C3′–O3′, O4′–C1′–C2′–O2′, and N–C1′–C2′–O2′) and the intrinsic anomeric effect of the heterocyclic base. As O4′–C4′–C3′–O3′ and O4′–C1′–C2′–O2′ gauche effects in **3** and **12–14** cancel each other, subtraction of $\Delta H°$ values for **3** from rN **12–14** gives an estimate for the combined anomeric effect of the base and gauche effect of the N–C1′–C2′–O2′ fragment: −6.2 kJ/mol for Ade (**12**), −4.6 kJ/mol for Gua (**13**) and +2.1 kJ/mol for Cyt (**14**). The subtraction of the values for the gauche effect of the N–C1′–C2′–O2′ fragment (see Level I) gives an estimate for the anomeric effect of adenine (+3.7 kJ/mol), guanine (+3.8 kJ/mol), and cytosine (+6.5 kJ/mol) bases in rN **12–14**. Note that the strengths of the individual anomeric effects are comparable in 2′,3′-ddN **6–8** and rN **12–14** with the reasonable assumption (see Level I) that the gauche effects of the O4′–C1′–C2′–O2′ and O4′–C4′–C3′–O3′ fragments are similar, while they are smaller in 2′-dN **9–11**. The difference in the estimates of the particular anomeric effects in 2′,3′-ddN, 2′-dN, and rN might be the result of (i) the reduction in the strength of the anomeric effect due to the change in the electrostatic potential around O4′ as it experiences the electron-withdrawing effects of 2′- and 2′/3′-OH groups or (ii) the errors in the pseudorotational analyses (*vide infra*), which are reflected in the values of $\Delta H°$. Alternatively, it can be also said that the strengths of the gauche effects (*vide supra*) are variable because the strength of the anomeric effect depends upon the nature of the aglycone. In 2′,3′-ddN **6–8**, the S conformers with the base in pseudoequatorial orientation have larger entropy. Approximately two-fold difference is noticed between the values of $\Delta S°$ for ddC (**8**) [12.7 ± 1.0 J/K·mol] to the values for ddA (**6**) [5.2 ± 0.6 J/K·mol] and ddG (**7**) [5.2 ± 0.7 J/K·mol] (Table IV).

Level III: Gauche Effect of [O4′–C4′–C3′–O3′] and Anomeric Effects. The changes in the pseudorotational equilibrium induced upon introduction of 3′-OH or a heterocyclic base at C1′ to abasic furanose system **1** have been assessed through comparison of conformational preferences in abasic sugars **1** and **2**, 2′,3′-ddN [ddA (**6**), ddG (**7**), ddC (**8**)], and 2′-dN [dA (**9**), dG (**10**), dC (**11**)]. It was suggested[3,11] that the population of the N and S conformers of dA (**9**) and other 2′-dN in D_2O solution changes only slightly with temperature (for dA (**9**) 25% N at 291 K and 27% N at 333 K[11]). The insensitivity of conformational equilibrium with respect to temperature would suggest that $\Delta H°$ of N ⇄ S conformational equilibrium is close to 0 and that the equilibrium is entropy driven.[3,11] However, the equilibrium populations of N and S conformers in 2′-dN change noticeably *within a larger temperature range* [for dA (**9**) 25% N at 278 K and 33% N at 358 K] (Table I), which is reflected in the non-zero values of $\Delta H°$ (Table IV). The enthalpy contribution [$\Delta H°$ = −4.2 ± 0.6 kJ/mol for dA (**9**), −2.5 ± 0.3 kJ/mol for dG (**10**), and −0.8 ± 0.4 kJ/mol for dC (**11**)] to $\Delta G°$ of N ⇄ S pseudorotational equilibrium in 2′-dN at 298 K is, in fact, *larger* than the contribution of entropy [$-T\Delta S°$ = 2.0 ± 0.7 kJ/mol for dA (**9**), 0.2 ± 0.2 kJ/mol for dG (**10**), and −0.5 ± 0.2 kJ/mol for dC (**11**)]. *In fact, in the cases of dA (**9**) and dG (**10**), it is the enthalpy contribution that drives the equilibrium to the S, whereas in terms of entropy, the N conformer is preferred (Table IV).*

The $\Delta H°$ values of N ⇄ S pseudorotational equilibrium in abasic sugars **1** and **2**, 2′,3′-ddN **6–8**, and 2′-dN **9–11** were dissected into following contributions: (i) the preference of the O4′–C4′–C3′–O3′ fragment for the gauche orientation, (ii) the anomeric effect of adenine base, (iii) the anomeric effect of guanine base, (iv) the anomeric effect of cytosine base, and (v) the substituent effect of the 5′-CH_2OH group. The regression analysis of those five unknowns (*i.e.*, stereoelectronic effects of substituents of the pentofuranose moiety) to eight experimentally determined

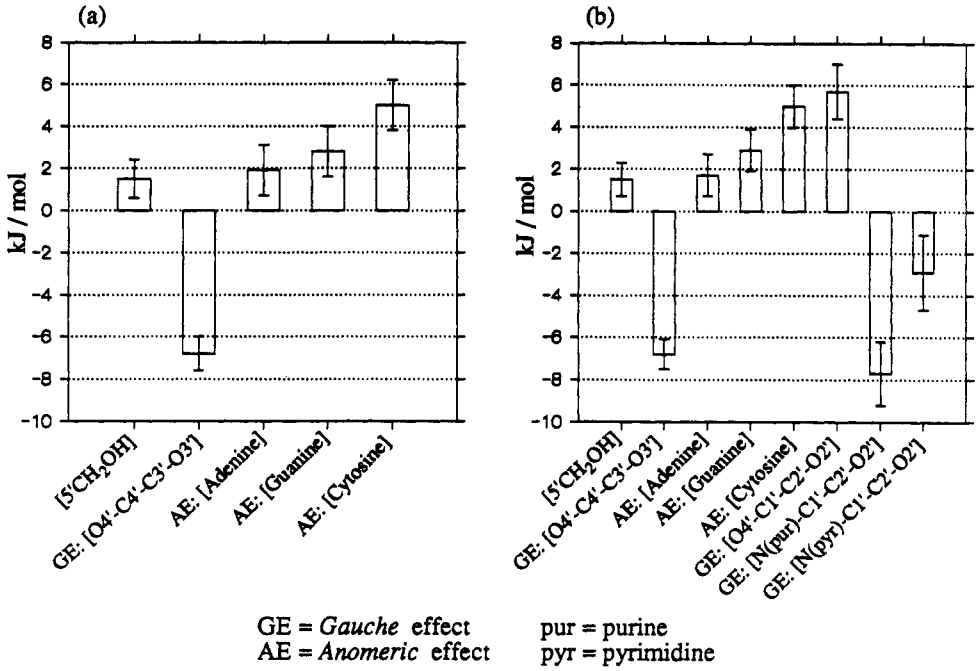

Figure 5. Relative contributions (in kJ/mol) of different gauche and anomeric effects to $\Delta H°$ of N ⇄ S conformational equilibrium. The positive sign means that the particular stereoelectronic effect prefers N-type conformation, while the minus sign denotes preference for the S-type. Both graphs represent the result of regression analyses described in the text. (a) The effect of [5′-CH_2OH] (+1.5 ± 0.9 kJ/mol), gauche effect of [O4′–C4′–C3′–O3′] (–6.8 ± 0.8 kJ/mol), anomeric effect of adenine (+1.9 ± 1.2 kJ/mol), anomeric effect of guanine (+2.8 ± 1.2 kJ/mol), and anomeric effect of cytosine +5.0 ± 1.2 kJ/mol bases on $\Delta H°$ of pseudorotational equilibrium in abasic sugars **1** and **2**, 2′, 3′-ddN **6–8**, and 2′-dN **9–11** (eq 2).[55] (b) The effect of [5′-CH_2OH] (+1.5 ± 0.8 kJ/mol), gauche effect of [O4′–C4′–C3′–O3′] (–6.8 ± 0.7 kJ/mol), anomeric effect of adenine (+1.7 ± 1.0 kJ/mol), anomeric effect of guanine (+2.9 ± 1.0 kJ/mol), anomeric effect of cytosine (+5.0 ± 1.0 kJ/mol) bases, gauche effect of [O4′–C1′–C2′–O2′] (+5.7 ± 1.3 kJ/mol), gauche effect of [$N_{(purine)}$–C1′–C2′–O2′] (–7.7 ± 1.5 kJ/mol), and gauche effect of [$N_{(pyrimidine)}$–C1′–C2′–O2′] (–2.9 ± 1.8 kJ/mol) on $\Delta H°$ of pseudorotational equilibrium in abasic sugars **1**, **2**, and **3**, 2′,3′-ddN **6–8**, 2′-dN **9–11**, and rN **12–14** (eq 3).[58]

$\Delta H°$ values (Table IV) gave a simple relationship (eq 2):[55,56]

$$\Delta H°\ (\text{kJ/mol}) = 1.5([5\text{-}CH_2OH]) - 6.8(\text{gauche effect [O4′–C4′–C3′–O3′]}) + 1.9(\text{anomeric effect [adenine]}) + 2.8(\text{anomeric effect[guanine]}) + 5.0(\text{anomeric effect [cytosine]}) \quad (2)$$

The positive sign in eq 2 implies that the particular stereoelectronic effect prefers N-type conformation, while the minus sign denotes preference for the S type. The appearance of the 3′-OH group drives the N ⇄ S equilibrium to S through the preference of the O4′–C4′–C3′–O3′ fragment to adopt a gauche rather than a trans orientation. The gauche effect of O4′–C4′–C3′–O3′ [–6.8 ± 0.8 kJ/mol] is the strongest factor in eq 2 (see also Figure 5a). The relative strength of the anomeric effect of purine bases (adenine [1.9 ± 1.2 kJ/mol] and guanine [2.8 kJ/mol (±1.2)]) is weaker in comparison with that of cytosine [5.0 kJ/mol (±1.2)]. The effect of 5′-CH_2OH group [+1.5 ± 0.9 kJ/mol] is the weakest stereoelectronic factor in eq 2 (Figure 5a) and denotes preference for N conformers. The errors in predicting the population of N and S conformers from the values of $\Delta H°$ calculated by eq 2 and $\Delta S°$ determined experimentally are given in Table V. The largest deviation between experimentally determined and predicted population of the N conformer within this set of eight compounds is 11% for **1** (column 5 in Table V). Certainly, the statistical significance of the values representing the anomeric effects is greatly improved as the number of knowns becomes larger than the number of unknowns (in comparison with Levels I and II). It is, however, noteworthy that eq 2 does not make any distinction between anomeric effects in 2′-dN **9–11** and 2′,3′-ddN **6–8**.

Level IV: Gauche and Anomeric Effects in 2′,3′-ddN, 2′-dN, and rN. In the abasic sugar **3** and rN [Ade (**12**), Gua (**13**), Cyt (**14**)] three gauche effects of O4′–C4′–C3′–O3′, O4′–C1′–C2′–O2′, and N–C1′–C2′–O2′ fragments are operating. It turned out that the single guache effect of N–C1′–C2′–O2′ cannot describe the conformational behavior of Ade (**12**) and Gua (**13**) in comparison with Cyt (**14**).[57] The higher preference for the N-type conformer in Cyt (**14**) in comparison with Ade (**12**) and Gua (**13**) (Table IV) suggests a specific interaction involving its carbonyl group[23,24] or other stereoelectronic effect that additionally contributes to the drive of the pseudorotational equilibrium. One probable explanation is that the nature of the base (*i.e.*, anomeric effect) also influences the strength of the preference for the gauche versus trans orientation of the N–C1′–C2′–O2′ fragment. The values of $\Delta H°$ for the N ⇄ S conformational equilibrium of

(55) The multiple *R*, equivalent to a Pearson correlation coefficient, is 0.984.[56] The values for tolerance, which is a measure of intercorrelation of parameters, are higher than 0.7 (a value near 0 would indicate that some of the predictors are highly interrcorrelated, which is an undesirable situation in regression).[56] The rms between predicted and experimental $\Delta H°$ values is 0.7 kJ/mol. In eq 2, the standard error[56] for the effect of the 5′-CH_2OH group is 0.9 kJ/mol; for the gauche effect of O4′–C4′–C3′–O3′, the standard error is 0.8 kJ/mol; and for all three anomeric effects, the standard error is 1.2 kJ/mol (Figure 5a).

(56) Wilkinson, L. *SYSTAT: The System for Statistics*; SYSTAT Inc.: 1989, Evanston, IL.

(57) The values of $\Delta H°$ for the pseudorotational equilibrium of the pentofuranose ring in abasic sugars **1–3**, 2′,3′-ddN **6–8**, 2′-dN **9–11**, and rN **12–14** were dissected into seven components: the preference of the O4′–C4′–C3′–O3′ (i), the O4′–C1′–C2′–O2′ (ii), and the N–C1′–C2′–O2′ (iii) fragments for the gauche orientation, anomeric effects of adenine (iv), guanine (v), or cytosine bases (vi), and the presence of the 5′-CH_2OH group (vii). Twelve data points were available to give the best fit through regression analysis to this model defined by seven unknowns.[56] The resulting equation was $\Delta H°$ (kJ/mol) = 1.5([5′-CH_2OH]) – 6.8(gauche effect[O4′–C4′–C3′–O3′]) + 1.2(anomeric effect[adenine]) + 2.3(anomeric effect[guanine]) + 6.0(anomeric effect[cytosine]) + 5.7 (gauche effect[O4′–C1′–C2′–O2′) – 6.1(gauche effect[N–C1′–C2′–O2′]). This model cannot describe the high preference of Cyt (**14**) for the N conformation, although the strength of the anomeric effect of cytosine base is predicted to be much stronger than the anomeric effect of adenine and guanine in comparison to the value predicted by eq 2. The difference between experimentally determined and modeled populations of the N conformer for Cyt (**14**) was 21%.

Table V. Populations of the N Conformers Calculated from the Values of $\Delta H°$ Predicted by Eqs 2 and 3 (see Scheme II)

compd	% N_{exp}[a] (298 K)	Level III (eq 2) $\Delta H°_{est}$[b] (kJ/mol)	% N_{est}[a,b]	Δ% N[c]	% N_{est}[b,d]	Δ% N[e]	Level IV (eq 3) $\Delta H°_{est}$[f] (kJ/mol)	% N_{est}[a,f]	Δ% N[g]	% N_{est}[d,f]	Δ% N[h]
1	51	1.5	62	−11	65	−14	1.5	62	−11	65	−14
2	25	−5.3	18	+7	11	+14	−5.3	18	+7	11	+14
ddA (**6**)	74	3.4	68	+6	80	−6	3.2	66	+8	78	−4
ddG (**7**)	75	4.3	75	0	85	−10	4.4	76	−1	86	−11
ddC (**8**)	78	6.5	75	+3	93	−15	6.5	75	+3	93	−15
dA (**9**)	29	−3.4	36	−7	20	+9	−3.6	34	−5	19	+10
dG (**10**)	29	−2.5	28	+1	27	+2	−2.4	29	0	28	+1
dC (**11**)	37	−0.3	42	−5	47	−10	−0.3	42	−5	47	−10
3	64						0.4	64	0	54	+10
Ade (**12**)	22						−5.6	24	−2	9	+13
Gua (**13**)	22						−4.4	20	+2	14	+8
Cyt (**14**)	69						2.5	69	0	73	−4

[a] The population of the N conformer was calculated through the relation % N = 100/[exp(−$\Delta G°/RT$) + 1]. $\Delta G° = \Delta H° - T\Delta S°_{exp}$, and R is the gas constant (8.314 J/K·mol). [b] The eq 2 was used to calculate the value of $\Delta H°_{est}$ (estimated), which was subsequently used to calculate % N. [c] Δ% N = (% N_{expt}, column 2) − (% N_{est}, column 4). [d] %N_{est} = 100/[exp(−$\Delta H°_{est}/RT$) + 1]. [e] Δ% N = (% N_{expt}, column 2) − (% N_{est}, column 6). [f] The values of $\Delta H°_{est}$ were calculated using eq 3. [g] Δ% N= (% N_{expt} column 2) − (% N_{est}, column 9). [h] Δ% N = (% N_{expt}, column 2) − (% N_{est}, column 11).

pentofuranose moieties in 2′,3′-ddN **6–8**, 2′-dN **9–11**, rN **12–14**, and abasic sugars **1**, **2**, and **3** were dissected into eight components: (i) the effect of 5′-CH_2OH group, (ii) the anomeric effects of the adenine base, (iii) the anomeric effects of the guanine, (iv) the anomeric effects of the cytosine base, (v) the gauche effect of O4′–C4′–C3′–O3′, (vi) the gauche effect of O4′–C1′–C2′–O2′, (vii) the gauche effect of $N_{(purine)}$–C1′–C2′–O2′, and (viii) the gauche effect of $N_{(pyrimidine)}$–C1′–C2′–O2′ fragments. The regression analysis of the 12 experimental $\Delta H°$ values (Table IV) for the description of the above eight unknowns (i–viii) gives eq 3.[58] The errors in predicting the population of N and S

$$\Delta H° \text{ (kJ/mol)} = 1.5([5'\text{-}CH_2OH]) - 6.8(\text{gauche effect}[O4'\text{–}C4'\text{–}C3'\text{–}O3']) + 5.7(\text{gauche effect}[O4'\text{–}C1'\text{–}C2'\text{–}O2']) + 1.7(\text{anomeric effect}[\text{adenine}]) + 2.9(\text{anomeric effect}[\text{guanine}]) + 5.0(\text{anomeric effect}[\text{cytosine}]) - 7.7(\text{gauche effect}[N_{(purine)}\text{-}C1'\text{-}C2'\text{-}O2']) - 2.9(\text{gauche effect}[N_{(pyrimidine)}\text{–}C1'\text{–}C2'\text{–}O2']) \quad (3)$$

conformers from $\Delta H°$ values calculated by the use of eq 3 are given in Table V. From the contributions of O–C–C–O fragments in eq 3 to $\Delta H°$ of pseudorotational equilibrium, it is clear that the preference of O4′–C4′–C3′–O3′ for the gauche orientation [−6.8 ± 0.7 kJ/mol] and therefore S sugar conformation is slightly stronger in comparison to the preference of O4′–C1′–C2′–O2′ fragment [+5.7 ± 1.3 kJ/mol] for the gauche orientation and N-type conformation.

The coefficients in eq 3 also suggest that the preference for gauche rather than trans orientation in N–C1′–C2′–O2′ fragments, which drives N ⇄ S equilibrium to the S, is greatly dependent on the nature of the glycosyl nitrogen atom. When the nitrogen atom is part of the purine ring, its preference for gauche orientation in the N–C1′–C2′–O2′ fragment is approximately 2.5 times stronger [−7.7 ± 1.5 kJ/mol] than when it is in pyrimidine [−2.9 ± 1.8 kJ/mol] (eq 3 and Figure 5b). The anomeric effect of cytosine base [+5.0 ± 1.0 kJ/mol] is much stronger than the anomeric effects of adenine [+1.7 ± 1.0 kJ/mol] or guanine [+2.9 ± 1.0 kJ/mol] bases.

Concluding Remarks

Conformational behavior of abasic sugars **1–3** and 2′,3′-ddN [ddA (**6**), ddG (**7**), ddC (**8**)], 2′-dN [dA (**9**), dG (**10**), dC (**11**)], and rN [Ade (**12**), Gua (**13**), Cyt (**14**)] in D_2O solution was studied through the analysis[2–4,8–16] of $^3J_{HH}$ coupling constants which were extracted from 500-MHz ^{1}H-NMR spectra recorded at 20 K intervals in the temperature range from 278 to 358 K (Table I). van't Hoff plots yielded $\Delta H°$ and $\Delta S°$ values of pseudorotational equilibria in abasic sugars **1–3** (Figure 3) and pentofuranose moieties in nucleosides **6–14** (Figure 4). The values of $\Delta H°$ and $\Delta S°$ have shown that the enthalpy contribution to $\Delta G°$ is larger than the contribution of entropy in abasic sugar **2** and nucleosides **6–14** (Table IV). It was therefore reasonable to assume that various stereoelectronic effects of substituents on the pentofuranose moiety are the main determinants for the drive of the pseudorotational equilibrium. The pseudorotational preferences in **1–14** observed in D_2O solution were described by simple quantification of gauche[39,40,45,46] and anomeric effects,[41,49] neglecting the minor changes of bond distances, bond angles, steric interactions, etc. between conformers participating in pseudorotational equilibrium. It has been shown through the comparison of conformational behavior of abasic sugars **1–3** that the substituent effect of the 5′-CH_2OH group is much weaker than the gauche effects of the O4′–C1′–C2′–O2′ and O4′–C4′–C3′–O3′ fragments. In **2**, the gauche effect of the O4′–C4′–C3′–O3′ fragment drives the N ⇄ S equilibrium to the S. Comparable values of $\Delta H°$ for the pseudorotational equilibrium in **1** and **3** show that the gauche effects of the O4′–C1′–C2′–O2′ and O4′–C4′–C3′–O3′ fragments are counteracting in their ability to drive the pseudorotational equilibrium and are of similar strength. The relative strengths of the gauche effects of the O4′–C4′–C3′–O3′ and O4′–C1′–C2′–O2′ fragments were further evaluated through the comparison of $\Delta H°$ values in abasic sugars **1**, **2**, and **3** with 2′,3′-ddN **6–8**, 2′-dN **9–11**, and rN **12–14**, respectively. The relative strengths of the gauche effects are different whether they are estimated through the comparison of abasic sugars **1–3** or nucleosides, which suggests that the strength of the gauche effect is correlated with the presence of other substituents, particularly the heterocyclic base at C1′. The comparison of $\Delta H°$ values between **1** and 2′,3′-ddN **6–8** has shown that the anomeric effect of cytosine is stronger in comparison with adenine and guanine bases. The anomeric effects in **6–8** can be interpreted as pure anomeric effects of the heterocycle. Analogous comparison of the values of $\Delta H°$ for N ⇄ S pseudorotational equilibrium in **2** and 2′-dN **9–11** shows a reduction in the strength of a particular anomeric effect. The preference for S-type conformations in 2′-dN **9–11** is due to the counteracting gauche effect of the O4′–C4′–C3′–O3′ fragment, which is stronger than the anomeric effect. In rN **12–14**, the anomeric effect is most probably even weaker in comparison with 2′-dN and 2′,3′-ddN, as O4′ experiences the inductive effect of the electron-withdrawing β-substituent operative through a

(58) The multiple R was 0.989 in this regression analysis.[56] The rms between modeled and experimental $\Delta H°$ values is 0.6 kJ/mol. In eq 3, the standard error for the effect of 5′-CH_2OH group is 0.8 kJ/mol; for the gauche effects of the O4′–C4′–C3′–O3′ and O4′–C1′–C2′–O2′ fragments, the standard errors are 0.7 and 1.3 kJ/mol, respectively; for all three anomeric effects, the standard error is 1.0 kJ/mol; for the gauche effect of $N_{(purine)}$–C1′–C2′–O2′, the standard error is 1.5 kJ/mol; and for the gauche effect of $N_{(pyrimidine)}$–C1′–C2′–O2′, the standard error is 1.8 kJ/mol (Figure 5b).[56]

σ-bond. The electron-withdrawing effect of the 3′-OH in the case of **9**–**11** and 2′- and 3′-OH in the case of **12**–**14** on O4′ lone pairs is clearly evident in the acid-promoted deglycosylation reaction. For example, the acid stability of adenine nucleosides increases in the following manner due to the decreased stability of the carboxonium ion[59] involving O4′–C1′: ddA (**6**) < dA (**9**) < Ade (**12**). Certainly, the estimation of individual anomeric effects would be greatly improved by the availability of high-quality parameters in the Karplus equation for the $-CH_2CH_2-$ fragment, which would increase the precision of pseudorotational analysis of (*S*)-tetrahydrofurfuryl alcohol (**1**) in particular. The conformational behavior in the complex system of rN **12**–**14** is additionally controlled by the gauche effect of the N–C1′–C2′–O2′ fragment, which drives the pseudorotational equilibrium to S-type conformations. It turned out that the differences in the conformational behavior of purine and pyrimidine rN can be described by the distinct nature of the glycosyl nitrogen atom and therefore the distinct strength of the gauche effect in $N_{(purine)}$–C1′–C2′–O2′ and $N_{(pyrimidine)}$–C1′–C2′–O2′ fragments.

Experimental Section

^{1}H-NMR Spectroscopy. ^{1}H-NMR spectra were recorded at 500 MHz for **1**–**14** in D_2O (10 mM) between 278 and 358 K at 20 K intervals. The analyses of ^{1}H-NMR spectra[60] of nucleosides and **2** were rather straightforward, whereas in the spectra of **1** and **3** some of the signals overlapped heavily. In **3**, H1″ overlaps with H3′, and H1′ overlaps with H5′. The ^{1}H-NMR spectrum of **3** was assigned by 1D ^{1}H NOE difference spectroscopy. Upon saturation of H2′ in **3**, NOE enhancements were observed at H3′/H1″ (8.7%), H5′/H1′ (0.8%), and H5″ (0.1%), which enabled the assignment of H1″. The main complication in the spectrum of **1** is severe overlap of the H3″, H2′, and H2″ signals (Figure 1). The ROESY spectrum (τ_m = 100 ms) showed the correlations between H2′ and H1″ and between H2″ and H1′. These two cross peaks are the basis for the assignment of protons at C1′. The protons at C2′ and C3′ were unequivocally assigned through the stereospecific deuteriation of H2″ and H3″. Figure 1 shows the disappearance of the signal for H2″ in **4** and the simplifications of the multiplets for the remaining protons. In a similar manner, the stereospecific deuteriation at C3′ in **5** has confirmed the assignment of H3′ and H3″ (Figure 1). The $^3J_{HH}$ and chemical shifts for **1**–**3** and **6**–**14** were obtained through the simulation and iteration procedure by the DAISY program package[60] (Table I).

Orientation around the C4′-C5′ Bond. The populations of the three staggered rotamers across C4′–C5′ (γ^+, γ^t, and γ^-) were calculated from $^3J_{4'5'}$ and $^3J_{4'5''}$ using a standard procedure[61] (Table I).

Conformational Analyses. We have developed the *A*, *B* parameter set in eq 1 specifically for **1**, **2**, and **3** through a set of *ab initio* calculations (Table II). These calculations were performed at the RHF/3-21G level both in vacuum and with SCRF (ϵ = 80).[51,22] The parameters *P* and Ψ_m are directly related to the set of endocyclic torsion angles ν_0[C4′–O4′–C1′–C2′], ν_1[O4′–C1′–C2′–C3′], ν_2[C1′–C2′–C3′–C4′], ν_3[C2′–C3′–C4′–O4′], and ν_4[C3′–C4′–O4′–C1′].[63] The conformational analyses of abasic sugars **1**, **2**, and **3** and nucleosides **6**–**14** have been performed with the program PSEUROT (version 5.4)[8-10,14-16] with the following relative electronegativities for the substituents present on the H–C–C–H fragment: in **1** for substituents around the C1′–C2′ bond, O4′ 1.40, C3′ 0.67, H 0.0, for substituents around the C2′–C3′ bond, C1′ 0.68, C4′ 0.62, H 0.0, and for substituents around the C3′–C4′ bond, C2′ 0.67, O4′ 1.40, C5′ 0.68; in **2** for substituents around the C1′–C2′ bond, C3′ 0.62, H 0.0, O4′ 1.40, for substituents around the C2′–C3′ bond, C1′ 0.68, H 0.0, OH 1.33, C4′ 0.62, and for substituents around the C3′–C4′ bond, C2′ 0.67, OH 1.33, O4′ 1.40, C5′ 0.68; in **3** for substituents around the C1′–C2′ bond, OH 1.33, C3′ 0.62, H 0.0, O4′ 1.40, for substituents around the C2′–C3′ bond, C1′ 0.68, OH 1.33, C4′ 0.62, and for substituents around the C3′–C4′ bond, C2′ 0.62, OH 1.33, O4′ 1.40, C5′ 0.68; in dA (**9**), dG (**10**), and dC (**11**) for substituents around the C1′–C2′ bond, H 0.0, C3′ 0.62, N atom of the base 0.82, O4′ 1.40, for substituents around the C2′–C3′ bond, C1′ 0.62, H 0.0, OH 1.33, C4′ 0.62, and for substituents around the C3′–C4′ bond, C2′ 0.67, OH 1.33, O4′ 1.40, C5′ 0.68; in Ade (**12**), Gua (**13**), and Cyt (**14**) for substituents around the C1′–C2′ bond, OH 1.33, C3′ 0.62, N of the base 0.82, O4′ 1.40, for substituents around the C2′–C3′ bond, C1′ 0.62, OH 1.33, C4′ 0.62, and for substituents around the C3′–C4′ bond, C2′ 0.62, OH 1.33, O4′ 1.40, C5′ 0.68. As noted above, five conformational parameters are needed to characterize a two-state pseudorotational equilibrium. Clearly, the number of unknowns is much smaller than the number of available 10 coupling constants in **1** ($^3J_{1'2'}$, $^3J_{1'2''}$, $^3J_{1''2'}$, $^3J_{1''2''}$, $^3J_{2'3'}$, $^3J_{2'3''}$, $^3J_{2''3'}$, $^3J_{2''3''}$, $^3J_{3'4'}$, and $^3J_{3''4'}$), which should greatly facilitate the pseudorotational analysis. The PSEUROT analysis without constraints predicts a 45% preference of the conformer characterized by P_N = −22°, Ψ_m = 32° over the *P* = 115°, Ψ_m = 48° conformer. The appearance of the E conformer in the two-state equilibrium was justified as a real minimum through a grid search (*vide supra*). Eight PSEUROT analyses of experimental $^3J_{HH}$ of **1** have been performed in which Ψ_m of both conformers were kept fixed in the range 35° < Ψ_m < 42° in 1-deg steps, and populations of conformers from those analyses were used in van't Hoff plots (Figure 3a). The discrepancies in the individual coupling constants between experimental values and $^3J_{HH}$ predicted by the PSEUROT were up to 1 Hz (Table III). The possible explanation lies in the fact that while electronegativity effects of O4′ on $^3J_{HH}$ are considered in the Karplus–Altona equation, the effect of bond angle changes around the pseudorotation pathway is neglected. It was recently shown by Barfield *et al.* that a small variation of bond angles in the H–C–C–H fragment can have a large influence on $^3J_{HH}$.[64] Another factor that influences the values of $^3J_{HH}$ is the "Barfield through-space transmission effect", which was originally used in the highly puckered envelope geometry of norbornanes to describe a relative decrease of the *endo–endo* cis coupling constant with respect to *exo–exo* cis coupling.[65] Trans couplings remain unaffected. In a five-membered ring, the Barfield transmission effect can be the reason for selective reduction of cis $^3J_{HH}$.[9,10,66] The main reason for the great discrepancies in $^3J_{HH}$ of **1** is probably a poorly parametrized Karplus equation. It goes without saying that the absence of a high-quality Karplus equation for CH_2CH_2 fragments (especially for $^3J_{HH}$ involving H1″) is also reflected in the result of the pseudorotational analysis of **1**. We have preformed PSEUROT analysis for **1** with eight coupling constants[54] ($^3J_{1'2'}$, $^3J_{1'2''}$, $^3J_{2'3'}$, $^3J_{2'3''}$, $^3J_{2''3'}$, $^3J_{2''3''}$, $^3J_{3'4'}$, and $^3J_{3''4'}$), and the resulting geometries suggest a N ⇄ E equilibrium, which was also established through the analysis of a complete vicinal *J* data set.[54] Only a few X-ray crystal structures of 1-deoxy sugar derivatives are known, and only one of five[50] suggests the existence of E conformers (*P* = 104.6°) due to the absence of the heterocyclic base at C1, while the other structures show the standard N (P_N = 18.6°) or S (P_S varies from 144° to 212°) conformations.[50] Recently, the report on the conformation of an α-L-arabinofuranoside moiety suggested an occurrence of E conformers in solution with *P* in the range from 57° to 70°.[5] The PSEUROT analysis of **2** (five unknowns, seven $^3J_{HH}$ at five temperatures) with no constraints showed a 75% preference for the S conformer at 298 K (P_N = 10°, Ψ_m = 31° and P_S = 138°, Ψ_m = 31°).[54] Six PSEUROT analyses of experimental $^3J_{HH}$ of **2** have been performed, in which Ψ_m values of both N and S conformers were kept fixed in the range 27° < Ψ_m < 32° in 1-deg steps. The populations of N and S conformers from those six analyses were used in van't Hoff plots (Figure 3b). The average ΔH° (−4.2 kJ/mol) is identical with the value obtained from the single PSEUROT analyses, described above with no constraints, while the average ΔS° (−5.2 J/K·mol) is within the error limits (Table

(59) Remaud, G.; Zhou, X.-X.; Chattopadhyaya, J.; Oivanen, M.; Lönnberg, H. *Tetrahedron* **1987**, *43*, 4453.

(60) Spin Simulation program (seven spins), DAISY, from Bruker was used.

(61) Haasnoot, C. A. G.; de Leeuw, F. A. A. M.; de Leeuw, H. P. M.; Altona, C. *Recl. Trav. Chim. Pays-Bas* **1979**, *98*, 576. Limiting values for $J_{4'5'}$ and $J_{4'5''}$ in the staggered C4′-C5′ rotamers are as follows: γ^+, $J_{4'5'}$ = 2.4 Hz, $J_{4'5''}$ = 1.3 Hz; rotamer γ^t, $J_{4'5'}$ = 2.6 Hz, $J_{4'5''}$ = 10.5 Hz; rotamer γ^-, $J_{4'5'}$ = 10.6 Hz, $J_{4'5''}$ = 3.8 Hz.

(62) A set of *ab initio* calculations was performed on **1**, **2**, and **3** at the RHF level using the 3-21G basis set. For each of the three compounds, two geometry optimizations were performed. The starting conformers of all three compounds were characterized by *P* = 0°, Ψ_m = 39° and *P* = 180°, Ψ_m = 39°. Completely free optimization of **1** converged to *P* = 16.0°, Ψ_m = 38.0° and *P* = 150.2°, Ψ_m = 38.9°. The N conformer was energetically preferred over the S by 3.0 kJ/mol. Similarly, two unconstrained optimizations of **2** converged to *P* = 27.1°, Ψ_m = 40.1° and *P* = 155.2°, Ψ_m = 42.0°. The S conformer was preferred by 0.9 kJ/mol. Two calculations on **3** converged to *P* = 18.1°, Ψ_m = 45.7° and *P* = 152.4°, Ψ_m = 42.1°. All *ab initio* calculations were performed with the use of the GAUSSIAN 92 program (ref 51) on SGI Indigo R4000. Typical CPU time for optimizations was 2–3 h for **1**, 3–4 h for **2**, and 6–7 h for **3**.

(63) The relationship between *P*, Ψ_m, and the five endocyclic torsion angles is simply $\nu_j = \Psi_m \cos(P + (j-2) \times 144°)$, with *j* = 0–4.

(64) Barfield, M.; Smith, W. B. *J. Am. Chem. Soc.* **1992**, *114*, 1574.

(65) Marshall, J.; Walter, S. R.; Barfield, M.; Marchand, A. P.; Marchand, N. W.; Serge, A. *Tetrahedron* **1976**, *32*, 537.

(66) Jaworski, A.; Ekiel, I.; Shugar, D. *J. Am. Chem. Soc.* **1978**, *100*, 4357.

Scheme III. Synthesis of Abasic Sugars **1–3** and Deuterated Derivatives **4** and **5**[a]

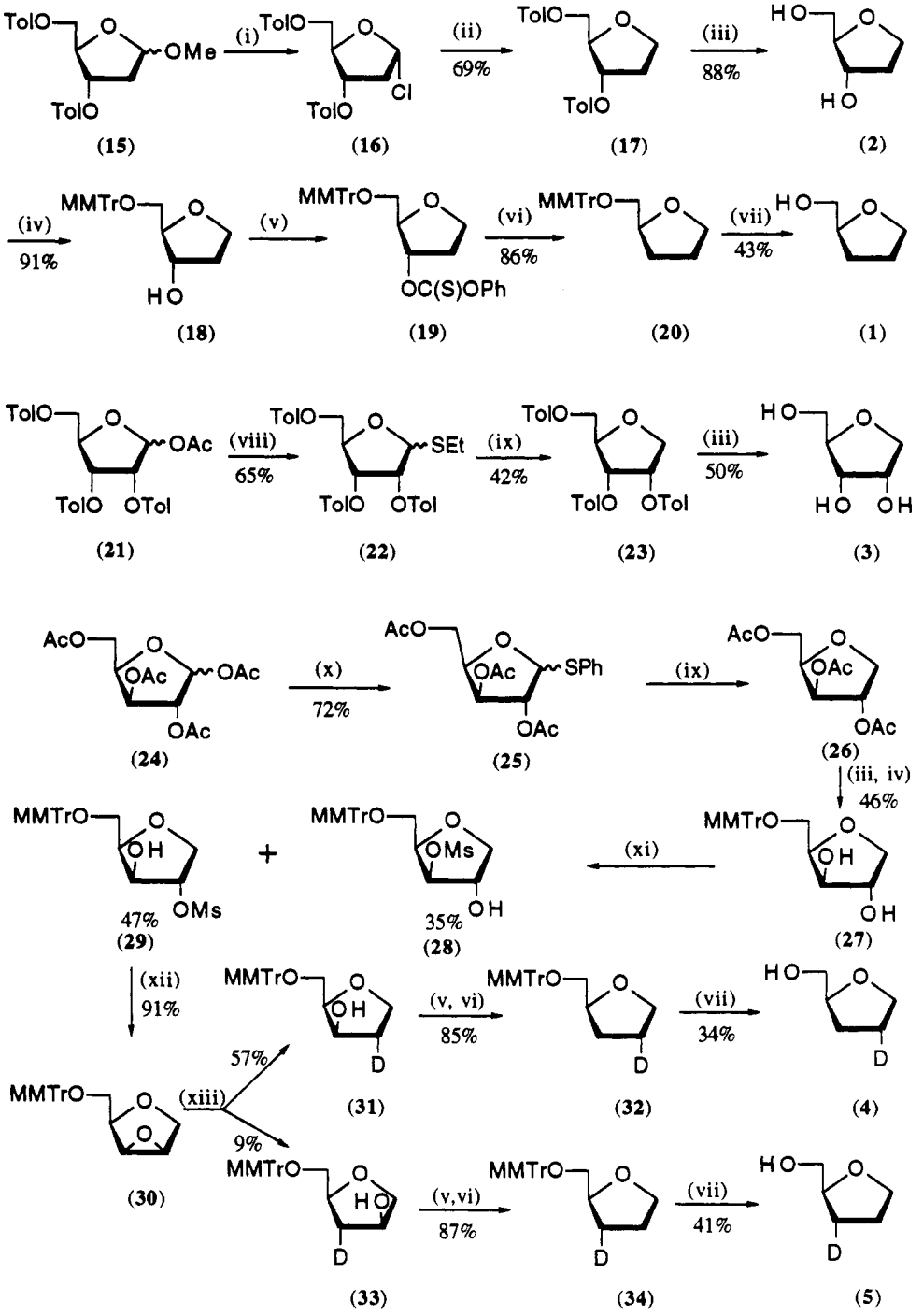

[a] Reagents: (i) AcOH, HCl; (ii) AIBN, Bu_3SnH, benzene, 80 °C; (iii) aqueous NaOH; (iv) MMTrCl, dry pyridine; (v) PhOC(S)Cl, DAMP, MeCN; (vi) AIBN, Bu_3SnH, toluene, 110 °C; (vii) CF_3COOH (2%) in CH_2Cl_2; (viii) EtSH, $ZnCl_2$, CH_2Cl_2; (ix) AIBN (4 equiv), Bu_3SnH (4 equiv), toluene, 110 °C; (x) PhSH, $ZnCl_2$, CH_2Cl_2; (xi) MsCl, dry pyridine; (xii) NaOMe, MeOH; (xiii) $LiAlD_4$, THF.

IV). Four $^3J_{HH}$ are available for the PSEUROT analysis of **3** (Table I). The optimization with no constraints showed an unnatural puckering of 73° for one of the conformers (P = 100°). A grid search procedure has been performed for **3**, which has shown that the conformational equilibrium can be described by $-16° < P_N < 3°$, $76° < P_S < 107°$, and $37° < \Psi_m < 42°$ (see supplementary material). Six PSEUROT analyses of experimental $^3J_{HH}$ of **3** have been performed, in which Ψ_m values of both conformers were kept fixed in the range $37° < \Psi_m < 42°$ in 1-deg steps. Populations of conformers from those analyses were used in van't Hoff plots (Figure 3c). The average $\Delta H°$ (+0.3 kJ/mol) and $\Delta S°$ (−3.8 J/K·mol) based on those six analyses are given Table IV. If $J_{1''2'}$ is, however, excluded from PSEUROT analysis, the following equilibrium is established: $P_N = 36°$, $\Psi_m = 32° \rightleftarrows P_{II} = 160°$, $\Psi_m = 38°$.[54] The N conformer is preferred by 87% at 293 K, and its population does not change with temperature. In the cases of Ade (**12**, Gua (**13**), and Cyt (**14**), only three vicinal couplings ($^3J_{1'2'}$, $^3J_{2'3'}$, and $^3J_{3'4'}$) are available. The coupling constants showed some change over a range of temperatures (Table I), and that facilitated conformational analysis. The PSEUROT analyses of Ade (**12**) and Gua (**13**) were performed by constraining the geometries of the minor N conformers to P = 9° and Ψ_m = 39°.[67] In the case of Cyt (**14**), the geometry of the minor S conformer was constrained to P = 161° and Ψ_m = 36°.[68] The results are presented in Table III. PSEUROT analyses of dA (**9**), dG (**10**), and dC (**11**), where five coupling constants are available ($^3J_{1'2'}$, $^3J_{1'2''}$, $^3J_{2'3'}$, $^3J_{2''3'}$, and $^3J_{3'4'}$) should be largely facilitated. Nevertheless, the geometry of the minor

(67) Lai, T. F.; Marsh, R. E. *Acta Crystallogr., Sect. B* **1972**, *28*, 1982.
(68) Thewalt, U.; Bugg, C. E.; Marsh, R. E. *Acta Crystallogr., Sect. B* **1970**, *26*, 1089.

N conformer was kept fixed in the analyses of dA (**9**), dG (**10**), and dC (**11**) (Table III).[12] The values of *P* and Ψ_m (Table III) in 2'-dN **9–11** and rN **12–14** determined through PSEUROT analyses (version 5.4) are slightly different compared to the values from X-ray crystallographic data.[4,67,68]

Chemical Syntheses. The synthesis of deoxy sugar derivatives on the nonanomeric position(s) is well documented.[69-75] The main synthetic approaches are (i) hydrolysis of glycals,[69,70] (ii) opening of epoxide by hydride ion,[71] (iii) degradation,[72] and (iv) reduction of thio sugars or free-radical reaction of thiocarbonyl derivatives.[73,74] To the best of our knowledge, the only report that has appeared on the synthesis of 1-deoxy sugar derivatives[75] deals with Raney nickel reduction of ethylthio-α-D-glucofuranoside to give the title compound.[75] 1-Chloro sugars are well established intermediates in the synthesis of nucleosides,[76,77] which we chose to be the precursor for making 1-deoxy sugar derivatives. The compounds **1** and **2** were prepared from 2-deoxy-D-ribose (Scheme III). The key intermediate **16** was prepared according to a literature method.[78] The free-radical reaction was used to reduce the 1-chloro derivative **16** with tributyltin hydride in the presence of AIBN to give 1-deoxy sugar **17** (70%). The ^{1}H-NMR spectrum showed that both H1 and H2 signals of 1-chloro derivative **16** moved upfield after reduction (H1 from δ 6.47 in **16** to δ 4.02 in **17** and H2 from δ 2.77 in **16** to δ 2.28 in **17**) and H1 region also gave the integral for two protons. The deprotection of compound **17** with 1 M sodium hydroxide gave fully deprotected 1,2-dideoxy-D-ribofuranose (**2**) (87%). The compound **2** was selectively protected with 4-monomethoxytrityl group to yield **18** (91%), which was converted to **19** by treatment with phenyl chlorothioformate. The intermediate **19** was reduced under a free-radical reaction condition to give **20** (86%). (*S*)-Tetrahydrofurfuryl alcohol (**1**) (42%) was obtained after removal of MMTr group in **20** with 2% trifluoroacetic acid in dichloromethane. The 1-deoxy-D-ribofuranose (**3**) was prepared from D-ribose (Scheme III). 1-Ethanethiolate derivative **22** was chosen as the intermediate instead of a 1-halo sugar due to the fact that the chloronation of protected D-ribose is very sluggish, taking 7–10 days for completion in the comparison with 2-deoxy sugar derivatives.[79] It is also difficult to isolate pure 1-chloro ribosugar derivatives because of their instability,[79,80] which makes it mandatory to perform the condensation reaction with the nucleobase only *in situ*.[79,80] Since the free-radical reaction should be performed on pure starting material, we have employed 1-thio sugar derivatives for the preparation of 1-deoxy sugar derivatives. The fully protected D-ribose derivative **21** was prepared according to the literature procedure.[79] The compound **21** was treated with ethanethiol in dichloromethane in the presence of zinc(II) chloride to give 1-ethylthio-2,3,5-tri-*O*-toluoyl-D-ribofuranose (**22**) (65%). The free-radical reduction could be driven to only a partial completion with tributyltin hydride (4 equiv) in the presence of a large amount of AIBN (4 equiv) in boiling toluene for 20 h to give the 1-deoxy sugar derivative **23** (41%) (approximately 20% of **22** was found unreacted). The final product 1-deoxy-D-ribofuranose (**3**) was obtained in 50% yield by deprotection of compound **23** with 1 M sodium hydroxide aqueous solution. Stereospecifically, deuterium-incorporated sugar derivatives are quite important because they simplify ^{1}H-NMR spectra enormously for compounds where multiple spin–spin couplings are involved, as in (*S*)-tetrahydrofurfuryl alcohol (**1**). The opening of epoxide is a useful method for the stereospecific synthesis of deuterated sugar derivatives and was reported by this lab[81] and other groups.[82] We have prepared the C4 (*R*) and C3 (*S*) deuterated analogues **4** and **5** of (*S*)-tetrahydrofurfuryl alcohol (**1**) in a stereospecific manner through the nucleophilic substitution reaction on the epoxide **30** (Scheme III). We chose to employ the 1-phenylthio derivative rather than the 1-ethylthio, because the phenylthio group is removed in a more facile manner. 1,2,3,5-Tetra-*O*-acetyl-D-xylofuranose (**24**)[83] was reacted with thiophenol under the acidic conditions to give compound **25** (72%). The thiolated compound **25** was reduced under the free-radical reaction conditions, acetyl groups were removed by 1 M aqueous sodium hydroxide, and 1-deoxy-D-xylofuranose was protected by the monomethoxytrityl group to give compound **27** (46%). The treatment of **27** with methanesulfonyl chloride in dry pyridine gave a mixture of 2- and 3-*O*-mesylated compounds which was purified to give **28** (35%) and **29** (47%). The *lyxo*-epoxide **30** was prepared by treatment of **29** with sodium methoxide in methanol (91%). The opening of the *lyxo*-epoxide **30** by lithium aluminium deuteride in dry THF gave a mixture of 5-*O*-(monomethoxytrityl)-1,2-dideoxy-2-(*S*)-deuterio-D-xylofuranose (**31**) (57%) and 5-*O*-(monomethoxytrityl)-1,3-dideoxy-3-(*S*)-deuterio-D-arabinofuranose (**33**) (9%). Both deuterated compounds **31** and **33** were converted to phenoxythiocarbonyl derivatives, which gave after free-radical reduction in toluene compounds **32** (85%) and **34** (87%), respectively. The deprotection of compounds **32** and **34** gave the deuterated **4** (34%) and **5** (41%), respectively.

Acknowledgment. We thank the Swedish Board for Technical Development and Swedish Natural Science Research Council, Swedish Board for Technical Development (NUTEK), and Medivir AB, Lunastigen 7, S-141 44 Huddinge, Sweden, for generous financial support. Thanks are due to the Wallenbergstiftelsen, Forskningrådsnämnden, and University of Uppsala for funds for the purchase of a 500-MHz Bruker AMX NMR spectrometer. The authors are indebted to Prof. Dr. C. Altona for the suggestion described in note 54 and to Mr. N. Puri for the measurement of the mass spectra.

Supplementary Material Available: Plots of correlation between proton–proton and corresponding endocyclic torsion angles (Figures 6–8), rms contours between experimental and calculated $^3J_{HH}$ values calculated for various geometries (P and Ψ_m) of N and S pseudorotamers (Figure 9), and experimental data for the chemical syntheses of abasic sugars **1–3** and deuterated derivatives **4** and **5** described in Scheme III (9 pages). Ordering information is given on any current masthead page.

(69) Zhdanov, Y. A.; Alexeeva, V. G. *Carbohydr. Res.* **1969**, *10*, 184.
(70) Vargha, C.; Kuszmann, J. *Chem. Ber.* **1963**, *96*, 2016.
(71) Taniguchi, M.; Koga, K.; Yamada, S. *Chem. Pharm. Bull.* **1974**, *22*, 2318.
(72) Sowden, J. C. *J. Am. Chem. Soc.* **1954**, *76*, 3541.
(73) Casini, G.; Goodman, L. *J. Am. Chem. Soc.* **1963**, *85*, 235.
(74) Drytakina, N. B.; Azhayev, A. V. *Synthesis* **1985**, 961.
(75) Huebner, C. F.; Link, K. P. *J. Biol. Chem.* **1950**, *186*, 387.
(76) Griengl, H. *J. Med. Chem.* **1985**, *28*, 1769.
(77) Nishimura, T.; Shimizu, B.; Iwai, I. *Chem. Pharm. Bull.* **1968**, *11*, 1470.
(78) Hoffer, M. *Chem. Ber.* **1960**, *93*, 2777.
(79) Kissman, H. M.; Pidacks, C.; Baker, B. R. *J. Am. Chem. Soc.* **1954**, *77*, 18.
(80) Schmidt, C. J.; Townsend, L. B. *J. Org. Chem.* **1972**, *37*, 2300.
(81) Pathak, T.; Bazin, H.; Chattopadhyaya, J. *Tetrahedron* **1986**, *42*, 5427.
(82) David, S.; Ustache, B. *Carbohydr. Res.* **1971**, *20*, 319.
(83) Holy, A. *Collect. Czech. Chem. Commun.* **1977**, *42*, 902.